Mon. Not. R. Astron. Soc. **000**, 000–000 (0000) Printed 2 February 2008 (MN LaTeX style file v1.4)

Electrodynamics of black hole magnetospheres

Komissarov S.S.
Department of Applied Mathematics, The University of Leeds, Leeds. E-mail: serguei@amsta.leeds.ac.uk

2 February 2008

ABSTRACT
The main goal of this research is to get better insights into the properties of the plasma filled magnetospheres of black holes by means of direct numerical simulations and, ultimately, to resolve the controversy surrounding the Blandford-Znajek mechanism. Driven by the need to write the equations of black hole electrodynamics in the form convenient for numerical applications, we constructed a new system of 3+1 equations which not only has more traditional form than now classical 3+1 system of Thorne and Macdonald but which is also more general. To deal with the magnetospheric current sheets, we also developed a simple model of radiative resistivity based on the inverse Compton scattering of background photons. The results of numerical simulations combined with simple analytical arguments allow us to make a number of important conclusions on the nature of the Blandford-Znajek mechanism. We show that, just like in the Penrose mechanism and in the MHD models of Punsly and Coroniti, the key role in this mechanism is played by the black hole ergosphere. The poloidal currents are driven by the gravitationally induced electric field which cannot be screened within the ergosphere by any static distribution of the electric charge of locally created pair plasma. Contrary to what is expected in the Membrane paradigm, the energy and angular momentum are extracted not only along the magnetic field lines penetrating the event horizon but along all field lines penetrating the ergosphere. In dipolar magnetic configurations symmetric relative to the equatorial plane the force-free approximation breaks down within the ergosphere where a strong current sheet develops along the equatorial plane. This current sheet supplies energy and angular momentum at infinity to the surrounding force-free magnetosphere. The Blandford-Znajek monopole solution is found to be asymptotically stable and causal. The so-called horizon boundary condition of Znajek is shown to be a regularity condition at fast critical surface.

Key words: black hole physics:general – magnetic fields – methods:numerical

1 INTRODUCTION

As the result of great advances in observational astrophysics during the previous several decades black holes are no longer regarded as peculiar solutions allowed by the Einstein equations which may or may not have anything to do with real astronomical phenomena. It is now widely believed that black holes are common in the Universe and play a key role in the most violent space events such as activity of galactic nuclei and gamma-ray bursts. Enormous amounts of energy released during such events can have two different origins. First of all this can be the gravitational energy of matter released during accretion onto an already existing black hole or during the gravitational collapse leading to formation of a new black hole. On the other hand, this can be the rotational energy of a black hole itself.

The notion of rotational energy of a black hole emerged as the result of theoretical discovery made by Penrose(1969) who found that a fraction of the Kerr hole mass can be converted, at least in principle, into the energy of surrounding matter or radiation (see also Cristodolou 1970). He has shown that two particles may interact in the neighbourhood of the black hole in such a way that one of the particles acquires negative energy and eventually disappears into the hole whereas the other particle carries away excessive positive energy. Unfortunately, as this was shown later, such interactions are rather special and must be very rare under typical astrophysical conditions, rendering the Penrose process inefficient (Bardeen et al. 1973). However, it was also found that the electromagnetic field can be used to extract the rotational energy of black holes too.

First, Goldreich and Julian(1969) analysed the vacuum solution for a rotating neutron star with a dipolar magnetic field aligned with the rotational axis. They argued that the rotationally induced electric field was strong enough to pull charged particles from the stellar surface and, thus, fill the

surrounding space with plasma. Using the force-free approximation to describe the produced magnetosphere they argued that an electromagnetically driven wind would carry away rotational energy and angular momentum of the star.

Then, Wald(1974) found a rather interesting particular solution of the vacuum Maxwell equations in the Kerr spacetime. Far away from the hole this solution described a uniform magnetic field aligned with the rotational axis of a black hole. However, near the black hole it described a strong electric field as well. Moreover, just like in the problem of an aligned rotator this "gravitationally induced" electric field had a significant component along the magnetic field. Bisnovatyi-Kogan and Ruzmaikin (1976) argued that, in the case of astrophysical black holes, a rather strong magnetic field of such kind can be generated in their accretion discs.

Finally, Blandford & Znajek (1977) realised that the similarity between the vacuum solution for a Kerr black hole and the vacuum solution for a rotating neutron star meant the possibility of electromagnetically driven wind from a rotating black hole, provided the space around the black hole could be filled with plasma. Moreover, they argued that, under the typical astrophysical conditions, the vacuum solutions were, in fact, unstable to cascade pair production, ensuring a plentiful supply of charged particles. Then they developed a general theory of force-free steady-state axisymmetric magnetospheres of black holes and found a perturbative solution for a slowly rotating black hole with monopole magnetic field. The key element of this solution was Znajek's "boundary condition" (Znajek 1977) imposed on the event horizon. As expected, this solution exhibited outgoing electromagnetic fluxes of energy and angular momentum. Moreover, the electromagnetic mechanism seemed to be very robust and the estimated power of the wind was high enough to explain the energetics of radio galaxies and quasars.

In their analysis, Blandford & Znajek (1977) used covariant equations of electrodynamics and operated with components of the electromagnetic field tensor and four-potential. Later, Thorne and Macdonald (Thorne & Macdonald 1982; Macdonald & Thorne 1982) developed a 3+1 approach, where the equations of black hole electrodynamics were written in more or less traditional form in terms of the spatial vectors of electric and magnetic field as measured by the so-called local fiducial observer (FIDO). In this work they adopted the system of coordinates due to Boyer and Lindquist(1967) which has a number of useful properties but also one important drawback. Just like the system of Schwarzschild coordinates, it is singular at the event horizon. As the result, the event horizon appears as a peculiar inner boundary of of physical space which required rather special treatment.

A number of authors studied the properties of electromagnetic field near the event horizon (Hanni & Ruffini 1973; Hajicek 1974; Znajek 1977,1978; Damour 1978) and gradually a picture emerged, according to which the event horizon could be treated as a rotating conducting surface with surface charges, surface currents, and a finite surface resistivity. This perfectly suited the quest of Thorne and Mackdonald for a new formulation of the black hole electrodynamics which would make it look similar to the classical electrodynamics. Surprisingly enough, the drawback of the Boyer-Lindquist coordinates seemed to turn into an advantage. This theory of the event horizon have made a great impact on the current perception of the Blandford-Znajek mechanism which is now widely associated with a mental picture of magnetic field lines originating from the horizon and being torqued by its rotation. It stimulated the development of The Membrane Paradigm (Thorne et al.1986) where the event horizon is attributed with a whole range of physical properties. However, one has to admit that, in spite of all its attractive simplicity and mathematical correctness, this construction is purely artificial. Moreover, it is rather worrying that the emphasis put on the role of the event horizon makes the Blandford-Znajek mechanism completely alien to the Penrose mechanism, where the key role is played by the black hole ergosphere.

The electrodynamic mechanism together with the horizon theory is now widely accepted by the astrophysical community. In great contrast to this mainstream trend, Punsly and Coroniti (Punsly & Coroniti 1990a; Punsly & Coroniti 1990b) and later Punsly (see the review in Punsly,2001) completely rejected both these theories. They argued that the event horizon cannot be regarded as a unipolar inductor because it is causally disconnected from the outgoing wind. Indeed, both the fast and the Alfvén waves generated at the event horizon can propagate only inwards and cannot effect the events in the outer space. The apparent lack of a proper unipolar inductor in the Blandford-Znajek solution and its reliance on Znajek's boundary condition made Punsly and Coroniti to conclude that this solution is nonphysical and structurally unstable. They developed completely different MHD models which seemed to be based on clearer physical ideas. In brief, they argue that gravity forces magnetospheric plasma to rotate inside the black hole ergosphere in the same sense as the black hole and that the magnetic field exhibits a similar rotation because it is "frozen" into this plasma.

Koide (2003) carried out MHD simulations of dipolar black hole magnetospheres with plasma energy-density only $1 \div 2$ order of magnitude smaller than the energy density of electromagnetic field. Although the numerical solution did not reached a steady state in these simulations, the obtained results seemed to indicate that in this regime the inertial effects accounted for approximately half of the extracted energy. However, in the black hole magnetospheres filled with plasma via pair production the characteristic number density of particles is given by the so-called Goldreich-Julian density (Goldreich & Julian 1969; Beskin et al.1991; Hirotani & Okamoto 1998). Under the typical conditions of supermassive black holes in AGNs, this corresponds to the mass density of pair plasma hardly exceeding 10^{-13} of the energy density of the electromagnetic field. Thus, even if the particle density is several orders of magnitude larger than the Goldreich-Julian one, the inertial effects are still expected to be negligibly small. Given the fact that, in such a degenerate regime, the full system of relativistic MHD presents a real challenge for numerical methods (see Komissarov, 2001a, Gammie et al., 2003), it is difficult not to conclude that the electrodynamic approach is more suitable. This is one of the reasons for the renewed interest towards the theory of force-free electrodynamics (Komissarov 2002a; Blandford 2002). (This does not mean that the pair production is the only possible way of plasma supply in the neighbourhood of astrophysical black holes and that the inertial effects are

always that small. For example, the coronas of black hole accretion discs are likely to be filled with dense plasma pulled from the disc surface.)

The recent numerical studies of the force-free magnetospheres of black holes added to the controversy surrounding the Blandford-Znajek mechanism. On one hand, they revealed the asymptotic stability of the Blandford-Znajek monopole solution (Komissarov 2001b) and, thus, raised doubts about the validity of the causality arguments by Punsly and Coroniti. On the other hand, the results for the dipolar magnetospheres questioned the virtues of the horizon theory as well. Indeen, they clearly indicated that the key role in the electrodynamic mechanism is played not by the black hole event horizon but by its ergosphere (Komissarov 2002b). Moreover, these simulations also revealed a certain deficiency of the force-free approximation as a dissipative current sheet was formed in the equatorial plane within the ergosphere.

This paper is an attempt to understand the nature of the electrodynamic mechanism and to resolve the controversy surrounding it. In Sec.II we show that the 3+1 equations of the black hole electrodynamics can be written in a more general and somewhat simpler form than in (Macdonald & Thorne 1982; Thorne & Macdonald 1982). In Sec.III the basic results for the force-free magnetospheres are rederived using the new 3+1 formulation. In order to handle the ergospheric current sheets, one has to go beyond the force-free approximation and consider the resistive electrodynamics. A model of resistivity based on the inverse Compton scattering of the background photons is described in Sec.IV. In Sec.V we present the results of numerical studies of the black hole magnetospheres obtained within the framework of resistive electrodynamics. The implications of these results for the perception of the Blandford-Znajek mechanism are discussed in Sec.VI. The more technical information about the properties of light surfaces, the properties of the Kerr-Schild coordinate system, and the details of our numerical method is presented in the Appendix.

Throughout this paper we adopt $(-+++)$ signature for the spacetime and assume that the Greek indices range from 0 to 3 and refer to spacetime tensors whereas the Latin ones range from 1 to 3 and refer to purely spatial tensors. In addition, we adopt such units that the speed of light and 4π do not appear in the equations of electrodynamics.

2 3+1 ELECTRODYNAMICS OF BLACK HOLE

Following Macdonald & Thorne (1982) we adopt the foliation approach to the 3+1 splitting of spacetime in which the time coordinate t parametrises a suitable filling of spacetime with space-like hypersurfaces described by the 3-dimensional metric tensor γ_{ij}. These hypersurfaces may be regarded as the "absolute space" at different instances of time t. Below we describe a number of useful results for further references. If $\{x^i\}$ are the spatial coordinates of the absolute space then

$$ds^2 = (\beta^2 - \alpha^2)dt^2 + 2\beta_i dx^i dt + \gamma_{ij} dx^i dx^j \tag{1}$$

where α is called the "lapse function" and $\boldsymbol{\beta}$ is the "shift vector". In this paper we consider only such coordinates that

$$\partial_t g_{\alpha\beta} = 0. \tag{2}$$

The 4-velocity of the local fiducial observer, 'FIDO', which can be described as being at rest in the absolute space, is

$$n_\mu = (-\alpha, 0, 0, 0). \tag{3}$$

The spatial components of the projection tensor, which is used to construct pure spatial tensors,

$$\gamma_{\alpha\beta} = g_{\alpha\beta} + n_\alpha n_\beta, \tag{4}$$

coincide with the components of the spatial metric γ_{ij}. Other useful results are

$$n^\mu = \frac{1}{\alpha}(1, -\beta^i), \tag{5}$$

$$g^{t\mu} = -\frac{1}{\alpha} n^\mu, \tag{6}$$

$$g = -\alpha^2 \gamma, \tag{7}$$

where

$$\beta^i = \gamma^{ij}\beta_j, \quad g = \det g_{\mu\nu}, \quad \gamma = \det \gamma_{ij}.$$

β^i are the components of the velocity of the spatial grid relative to the local FIDO as measured using the coordinate time t and the spatial basis $\{\partial_i\}$ (Macdonald & Thorne 1982).

Landau and Lifshitz (1951) proposed a different approach to the 3+1 splitting of spacetime which is known as the congruence approach. They also showed that within this approach the covariant equations of electrodynamics in gravitational field can be reduced to a set of 3+1 equations very similar to the usual Maxwell equations in matter (e.g. Landau and Lifshitz, 1971).

The 3+1 electrodynamics of black holes within the foliation approach was developed by Thorne and Macdonald (1982) who used as a starting point the results by Ellis(1973) on the 3+1 electrodynamics in the congruence language. In fact, they derived rather general 3+1 integral equations of electrodynamics as well as the differential equations adapted to a particular foliation of the Kerr space-time, namely the Boyer-Lindquist foliation. This formulation has been used successfully in various theoretical studies of black hole electrodynamics. However, the Boyer-Lindquist foliation has one important disadvantage – it leads to the well known coordinate singularity at the event horizon. This singularity is removed in a different less known foliation, namely the Kerr-Schild foliation, which otherwise shares many common properties with the Boyer-Lindquist foliation (see Appendix B). It has been shown that the Kerr-Schild coordinates do not only simplify theoretical analysis but also allow to overcome a number of problems concerning numerical simulations (e.g. Papadopoulos & Font,1998, Komissarov, 2001). The corresponding set of 3+1 differential equations of electrodynamics is somewhat different. Moreover, in order to construct a Godunov type numerical scheme one needs a different type of integral equations compared to those given in Thorne and Macdonald (1982). All these equations can be obtained from the 3+1 integral equations of (Macdonald & Thorne 1982). However, they can also be derived directly from the covariant Maxwell equations, and so easily, that this is worth to be shown (see also Landau & Lifshitz, 1971; Koide, 2003).

The covariant Maxwell equations are (e.g. Jackson(1975)):

$$\nabla_\beta {}^*F^{\alpha\beta} = 0, \tag{8}$$

$$\nabla_\beta F^{\alpha\beta} = I^\alpha, \tag{9}$$

where $F^{\alpha\beta}$ is the Maxwell tensor of the electromagnetic field, ${}^*F^{\alpha\beta}$ is the Faraday tensor and I^α is the 4-vector of the electric current. The most direct way of 3+1 splitting of the covariant Maxwell equations is to write them down in components and then to introduce such spatial vectors that these equations have a particularly simple and familiar form. For example, when eq.(8) is written in components it splits into two parts:

- The time part:

$$\frac{1}{\sqrt{\gamma}}\partial_i\left(\alpha\sqrt{\gamma}\,{}^*F^{ti}\right) = 0, \tag{10}$$

- The spatial part:

$$\frac{1}{\sqrt{\gamma}}\partial_t\left(\alpha\sqrt{\gamma}\,{}^*F^{jt}\right) + \frac{1}{\sqrt{\gamma}}\partial_i\left(\alpha\sqrt{\gamma}\,{}^*F^{ji}\right) = 0, \tag{11}$$

If we now introduce the spatial vectors $\boldsymbol{B}$ and $\boldsymbol{E}$ via

$$B^i = \alpha\,{}^*F^{it} \tag{12}$$

$$E^i = \gamma^{ij}E_j, \quad E_i = \frac{\alpha}{2}e_{ijk}\,{}^*F^{jk}, \tag{13}$$

where $e_{ijk} = \sqrt{\gamma}\epsilon_{ijk}$ is the Levi-Civita pseudo-tensor of the absolute space, then equations (10,11) read

$$\boldsymbol{\nabla}\cdot\boldsymbol{B} = 0, \tag{14}$$

$$\partial_t\boldsymbol{B} + \boldsymbol{\nabla}\times\boldsymbol{E} = 0, \tag{15}$$

where ∇ is the covariant derivative of the absolute space. Notice, that in order to derive eq.(15) we used the stationarity condition (2). Similarly, equation (9) splits into

$$\boldsymbol{\nabla}\cdot\boldsymbol{D} = \rho, \tag{16}$$

$$-\partial_t\boldsymbol{D} + \boldsymbol{\nabla}\times\boldsymbol{H} = \boldsymbol{J} \tag{17}$$

where

$$D^i = \alpha F^{ti}, \tag{18}$$

$$H^i = \gamma^{ij}H_j, \quad H_i = \frac{\alpha}{2}e_{ijk}F^{jk}. \tag{19}$$

$$\rho = \alpha I^t, \quad J^k = \alpha I^k. \tag{20}$$

As one can see, these 3+1 equations have exactly the same form as the classical Maxwell equations for the electromagnetic field in matter. Applying ∇ to eq.(17) and then using eq.(16) one obtains the electric charge conservation law

$$\partial_t\rho + \boldsymbol{\nabla}\cdot\boldsymbol{J} = 0. \tag{21}$$

Similar to any highly ionized plasma, the pair plasma of black hole magnetospheres has essentially zero electric and magnetic susceptibilities. In such a case, the Faraday tensor is simply dual to the Maxwell tensor

$${}^*F^{\alpha\beta} = \frac{1}{2}e^{\alpha\beta\mu\nu}F_{\mu\nu} \tag{22}$$

$$F^{\alpha\beta} = -\frac{1}{2}e^{\alpha\beta\mu\nu}\,{}^*F_{\mu\nu}. \tag{23}$$

Here

$$e_{\alpha\beta\mu\nu} = \sqrt{-g}\,\epsilon_{\alpha\beta\mu\nu}, \tag{24}$$

is the Levi-Civita alternating pseudo-tensor of spacetime and $\epsilon_{\alpha\beta\mu\nu}$ is the four-dimensional Levi-Civita symbol. This allows to obtain the following alternative expressions for $\boldsymbol{B}, \boldsymbol{E}, \boldsymbol{D}$, and $\boldsymbol{H}$:

$$B^i = \frac{1}{2}e^{ijk}F_{jk} \tag{25}$$

$$E_i = F_{it}, \tag{26}$$

$$D^i = \frac{1}{2}e^{ijk}\,{}^*F_{jk}, \tag{27}$$

$$H_i = {}^*F_{ti}. \tag{28}$$

Moreover, from the above definitions one immediately finds the following vacuum constitutive equations:

$$\boldsymbol{E} = \alpha\boldsymbol{D} + \boldsymbol{\beta}\times\boldsymbol{B}, \tag{29}$$

$$\boldsymbol{H} = \alpha\boldsymbol{B} - \boldsymbol{\beta}\times\boldsymbol{D}. \tag{30}$$

At infinity, provided the coordinate system becomes Lorentzian there, one has $\alpha = 1$, $\beta = 0$ and, hence,

$$\boldsymbol{B} = \boldsymbol{H}, \qquad \boldsymbol{E} = \boldsymbol{D}.$$

One can easily obtain the following covariant forms of definitions (12,13,18,19,20):

$$B^\mu = -\,{}^*F^{\mu\nu}n_\nu, \tag{31}$$

$$E^\mu = -\frac{1}{2}\gamma^{\mu\nu}e_{\nu\alpha\beta\gamma}k^\alpha\,{}^*F^{\beta\gamma}, \tag{32}$$

$$D^\mu = F^{\mu\nu}n_\nu, \tag{33}$$

$$H^\mu = -\frac{1}{2}\gamma^{\mu\nu}e_{\nu\alpha\beta\gamma}k^\alpha F^{\beta\gamma}, \tag{34}$$

$$J^\mu = 2I^{[\nu}k^{\mu]}n_\nu, \tag{35}$$

$$\rho = -I^\nu n_\nu, \tag{36}$$

where $k^\alpha = \partial_t$. All these spacetime vectors are purely spatial, that is they have zero time component.

In terms of four-potential $\mathcal{U}_\mu$ one has

$$F_{\mu\nu} = -2\mathcal{U}_{[\mu,\nu]}.$$

Introducing the scalar potential Φ and the vector potential $\boldsymbol{A}$ as

$$\Phi = -\mathcal{U}_t, \tag{37}$$

$$A^i = \gamma^{ij}A_i, \quad A_i = \mathcal{U}_i \tag{38}$$

one obtains the familiar looking results

$$\boldsymbol{E} = -\nabla\Phi - \partial_t\boldsymbol{A}, \tag{39}$$

$$\boldsymbol{B} = \boldsymbol{\nabla}\times\boldsymbol{A}. \tag{40}$$

The covariant definitions are

$$A^\mu = \gamma^{\mu\nu}\mathcal{U}_\nu, \quad \Phi = -\mathcal{U}_\mu k^\mu.$$

From the covariant equation of motion for a particle with the four-velocity u^ν, the four-momentum p^μ, and the electric charge q,

$$\frac{Dp_\mu}{D\tau} = qF_{\mu\nu}u^\nu, \tag{41}$$

one easily obtains the following energy equation

$$\frac{de_p}{dt} = q\boldsymbol{E}\cdot\boldsymbol{v}, \tag{42}$$

where $e_p = -p_t$ is known as the "energy at infinity" and $v^i = dx^i/dt$ is the spatial velocity vector.

Both in the Boyer-Lindquist and the Kerr-Schild coordinates, where $\partial_\phi g_{\nu\mu} = 0$, one has an equally simple result for the angular momentum at infinity, $l_p = p_\phi$,

$$\frac{dl_p}{dt} = q(\boldsymbol{E} + \boldsymbol{v}\times\boldsymbol{B})\cdot\boldsymbol{m}, \tag{43}$$

where $\boldsymbol{m} = \partial_\phi$.

In terms of Maxwell tensor the electromagnetic stress-energy-momentum tensor is

$$T^\mu_{\ \nu} = F^{\mu\gamma}F_{\nu\gamma} - \frac{1}{4}(F_{\gamma\beta}F^{\gamma\beta})\delta^\mu_{\ \nu}. \tag{44}$$

In terms of $\boldsymbol{B}$,$\boldsymbol{E}$,$\boldsymbol{H}$, and $\boldsymbol{D}$ we have

$$T^t_{\ t} = -\frac{1}{2\alpha}(\boldsymbol{E}\cdot\boldsymbol{D} + \boldsymbol{B}\cdot\boldsymbol{H}), \tag{45}$$

$$T^i_{\ t} = -\frac{1}{\alpha}e^{ijk}E_jH_k, \tag{46}$$

$$T^t_{\ i} = \frac{1}{\alpha}e_{ijk}D^jB^k \tag{47}$$

$$T^i_{\ j} = -\frac{1}{\alpha}(D^iE_j + B^iH_j) + \frac{1}{2\alpha}(\boldsymbol{E}\cdot\boldsymbol{D} + \boldsymbol{B}\cdot\boldsymbol{H})\delta^i_j. \tag{48}$$

The covariant energy-momentum equation is

$$\nabla_\nu T^\nu_{\ \mu} = -F_{\mu\gamma}I^\gamma. \tag{49}$$

Both in the Boyer-Lindquist and in the Kerr-Schild coordinates, as in any other coordinates with cyclic coordinate ϕ such that $\partial_t g_{\mu\nu} = \partial_\phi g_{\mu\nu} = 0$, 3+1 splitting of eq.(49) leads to the following energy

$$\partial_t e + \boldsymbol{\nabla}\cdot\boldsymbol{S} = -(\boldsymbol{E}\cdot\boldsymbol{J}), \tag{50}$$

and the angular momentum

$$\partial_t l + \boldsymbol{\nabla}\cdot\boldsymbol{L} = -(\rho\boldsymbol{E} + \boldsymbol{J}\times\boldsymbol{B})\cdot\boldsymbol{m}, \tag{51}$$

equations for the electromagnetic field. Here

$$e = -\alpha T^t_{\ t} = \frac{1}{2}(\boldsymbol{E}\cdot\boldsymbol{D} + \boldsymbol{B}\cdot\boldsymbol{H}) \tag{52}$$

is the volume density of energy at infinity,

$$l = \alpha T^t_{\ \phi} = (\boldsymbol{D}\times\boldsymbol{B})\cdot\boldsymbol{m} \tag{53}$$

is the volume density of angular momentum at infinity,

$$\boldsymbol{S} = \boldsymbol{E}\times\boldsymbol{H} \tag{54}$$

is the flux of energy at infinity, and

$$\boldsymbol{L} = -(\boldsymbol{E}\cdot\boldsymbol{m})\boldsymbol{D} - (\boldsymbol{H}\cdot\boldsymbol{m})\boldsymbol{B} + \frac{1}{2}(\boldsymbol{E}\cdot\boldsymbol{D} + \boldsymbol{B}\cdot\boldsymbol{H})\boldsymbol{m} \tag{55}$$

is the flux of angular momentum at infinity.

It is well known that evolution equations like (15) and (17) can be written as conservation laws. In our case we obtain

$$\partial_t B^i + \nabla_j K^{ij} = 0, \tag{56}$$

and

$$\partial_t D^i + \nabla_j L^{ij} = -J^i, \tag{57}$$

where

$$K^{ij} = e^{ijk}E_k \quad \text{and} \quad L^{ij} = -e^{ijk}H_k. \tag{58}$$

are the magnetic and the electric field flux tensors. The corresponding integral equations are now easily obtained using the divergence theorem

$$\frac{d}{dt}\int_V B^i dV + \int_{\delta V} K^{ij}dS_j = 0, \tag{59}$$

$$\frac{d}{dt}\int_V D^i dV + \int_{\delta V} L^{ij}dS_j = -\int_V J^i dV, \tag{60}$$

where δV is the closed boundary of the spatial volume V; $dV = \sqrt{\gamma}dx^1dx^2dx^3$ is the infinitesimal metric volume of the absolute space, and $dS_i = e_{ijk}dx^j_{(1)}dx^k_{(2)}$ is the infinitesimal metric surface element of δV. One can see that both the differential and the integral 3+1 equations of black hole electrodynamics are, in fact, very similar to the corresponding equations of Minkowski spacetime. This suggests that many well known techniques can, almost readily, be used to solve this equations numerically.

In (Macdonald & Thorne 1982; Thorne et al.1986) the 3+1 equations of electrodynamics are written in terms of the electric and the magnetic field vectors as measured by the local FIDO. We denote this vectors as $\check{\boldsymbol{E}}$ and $\check{\boldsymbol{B}}$. From definitions (33,31) it follows that

$$\check{\boldsymbol{B}} = \boldsymbol{B} \quad \text{and} \quad \check{\boldsymbol{E}} = \boldsymbol{D}. \tag{61}$$

The main benefit gained by the introduction of FIDOs and, hence, the quantities measured by these observers, comes from the principle of equivalence. These observers can be treated as locally inertial observers and in their frames all local physical phenomena are governed by the laws of special relativity. For example, in order to close the system of Maxwell equations we need an additional constitutive equation relating the electric current to the electromagnetic field, namely the Ohm law. Thanks to the principle of equivalence, this can be done in terms of quantities measured by FIDOs, in the same way as in the special relativistic electrodynamics. From equation (36) it follows that ρ is, in fact, the electric charge density as measured by FIDOs. As shown in (Thorne & Macdonald 1982) the electric current density as measured by FIDOs, $\boldsymbol{j}$, is related to $\boldsymbol{J}$ via

$$\boldsymbol{J} = \alpha\boldsymbol{j} - \rho\boldsymbol{\beta}. \tag{62}$$

The second term in this equation accounts for the motion of spatial grid relative to FIDO.

In the Boyer-Lindquist coordinates $\boldsymbol{\nabla}\cdot\boldsymbol{\beta} = 0$, and under this condition equations (14,15,16,17) reduce to the corresponding equations in (Macdonald & Thorne 1982; Thorne et al.1986). For example, using equations (29,14) one finds that

$$\boldsymbol{\nabla}\times\boldsymbol{E} = \boldsymbol{\nabla}\times\boldsymbol{\alpha}\check{\boldsymbol{E}} - \mathcal{L}_{\boldsymbol{\beta}}\check{\boldsymbol{B}}, \tag{63}$$

where

$$\mathcal{L}_{\boldsymbol{\beta}}\check{\boldsymbol{B}} = (\boldsymbol{\beta}\cdot\boldsymbol{\nabla})\check{\boldsymbol{B}} - (\check{\boldsymbol{B}}\cdot\boldsymbol{\nabla})\boldsymbol{\beta} \tag{64}$$

is the Lie derivative of $\check{\boldsymbol{B}}$ along $\boldsymbol{\beta}$. Thus, equation (15) reads

$$\partial_t\check{\boldsymbol{B}} - \mathcal{L}_{\boldsymbol{\beta}}\check{\boldsymbol{B}} + \boldsymbol{\nabla}\times\boldsymbol{\alpha}\check{\boldsymbol{E}} = 0, \tag{65}$$

which is equation (3.52) in Thorne et al.(1986). However, in other coordinate systems, e.g. the Kerr-Schild system, $\boldsymbol{\nabla}\cdot\boldsymbol{\beta} \neq 0$.

The results presented in this section show that the 3+1 equations of black hole electrodynamics can be written in

a more general and much simpler form than in (Thorne & Macdonald 1982; Macdonald & Thorne 1982). Our equations are remarkably similar to the familiar equations of electrodynamics in matter. All effects of gravity are hidden in the constitutive equations 29,30) and in the spatial metric γ_{ij}.

3 STEADY-STATE FORCE-FREE MAGNETOSPHERES OF BLACK HOLES

In this section we re-derive, within our 3+1 framework, some of the well known results for the steady-state force-free magnetospheres of black holes obtained by Blandford & Znajek(1977). The only condition imposed on the coordinate system is $\partial_\phi g_{\nu\mu} = \partial_t g_{\mu\nu} = 0$ and, thus, these results hold equally well both in the Boyer-Lindquist and the Kerr-Schild coordinates.

The covariant force-free condition

$$F_{\mu\nu} I^\mu = 0$$

can be written in the 3+1 language as

$$\boldsymbol{E}\cdot\boldsymbol{J} = 0, \tag{66}$$

and

$$\rho\boldsymbol{E} + \boldsymbol{J}\times\boldsymbol{B} = 0, \tag{67}$$

or

$$\boldsymbol{D}\cdot\boldsymbol{j} = 0, \tag{68}$$

and

$$\rho\boldsymbol{D} + \boldsymbol{j}\times\boldsymbol{B} = 0. \tag{69}$$

From eq.(69) it follows that

$$\boldsymbol{D}\cdot\boldsymbol{B} = \check{\boldsymbol{E}}\cdot\check{\boldsymbol{B}} = 0, \tag{70}$$

and

$$\boldsymbol{j}_\perp = \rho\frac{\boldsymbol{D}\times\boldsymbol{B}}{B^2} = \rho\frac{\check{\boldsymbol{E}}\times\check{\boldsymbol{B}}}{\check{B}^2}, \tag{71}$$

where $\boldsymbol{j}_\perp$ is the component of electric current normal to $\boldsymbol{B}$. Equation (71) states that this component is entirely due to the drift motion of charged particles. Since the drift velocity must be lower than the speed of light we have

$$B^2 - D^2 > 0 \quad \text{or} \quad \check{B}^2 - \check{E}^2 > 0. \tag{72}$$

Equations (70) and (72) are the 3+1 representations of the Lorentz invariant constraints of force-free approximation

$${}^*F_{\mu\nu}F^{\mu\nu} = 0 \quad \text{and} \quad F_{\mu\nu}F^{\mu\nu} > 0$$

(Znajek 1977; Komissarov 2002a). Whereas the constraint (70) is automatically satisfied by any force-free steady-state solution, the constraint (72) is not and, hence, it always has to be checked (Znajek 1977). If this condition is not satisfied the Alfvén wavespeed becomes complex and, thus, the system of force-free electrodynamics (magnetodynamics seems to be a better name) is no longer hyperbolic (Komissarov 2002a). The physical reason why the force-free approximation breaks down if $\boldsymbol{E}\cdot\boldsymbol{B} = 0$ but $B^2 - E^2 < 0$ is quite obvious. Under such conditions, one can find a local inertial frame where the electromagnetic field is seen as a pure electric field.

The conditions of axisymmetry and time-independency imply that

$$E_\phi = \mathcal{U}_{t,\phi} - \mathcal{U}_{\phi,t} = 0. \tag{73}$$

Given this, equation (67) ensures that

$$\boldsymbol{J}_p \parallel \boldsymbol{B}_p, \quad \boldsymbol{E}_p \perp \boldsymbol{B}_p, \tag{74}$$

where index p refers to the poloidal component of a vector. These show that there exists a purely azimuthal vector $\boldsymbol{\omega} = \Omega\partial_\phi$ such that

$$\boldsymbol{E} = -\boldsymbol{\omega}\times\boldsymbol{B} \tag{75}$$

and

$$\boldsymbol{D} = -\frac{1}{\alpha}(\boldsymbol{\omega} + \boldsymbol{\beta})\times\boldsymbol{B}. \tag{76}$$

Substituting (75) into the stationary version of (15), one finds

$$\boldsymbol{\nabla}\times(\boldsymbol{\omega}\times\boldsymbol{B}) = 0,$$

which leads to

$$\boldsymbol{B}\cdot\nabla\Omega = 0. \tag{77}$$

Thus, Ω, which is called the angular velocity of magnetic field, is constant along the magnetic field lines.

From equations (17) and (74) it immediately follows that

$$B^\theta\partial_\theta H_\phi + B^r\partial_r H_\phi = 0, \tag{78}$$

and, thus, H_ϕ is also constant along the magnetic field lines (This constant is denoted as B_T in Blandford & Znajek,1977.)

Another parameter constant along the magnetic field lines is the scalar potential, which we denote as Φ. Indeed, from eqs.(39,75) one immediately finds that

$$\boldsymbol{B}\cdot\boldsymbol{\nabla}\Phi = 0. \tag{79}$$

Since the source terms in eqs.(50,51) vanish, the energy and the angular momentum of the electromagnetic field are conserved.

$$\partial_t e + \boldsymbol{\nabla}\cdot\boldsymbol{S} = 0, \tag{80}$$

$$\partial_t l + \boldsymbol{\nabla}\cdot\boldsymbol{L} = 0. \tag{81}$$

Substituting $\boldsymbol{E}$ from (75) into eq.(55) and eq.(54) one obtains the following expressions for the poloidal component of the angular momentum flux vector

$$\boldsymbol{L}_p = -H_\phi\boldsymbol{B}_p, \tag{82}$$

and the poloidal component of the energy flux vector

$$\boldsymbol{S}_p = -(H_\phi\Omega)\boldsymbol{B}_p, \tag{83}$$

where $\boldsymbol{B}_p$ is the poloidal component of the magnetic field. Thus, both the energy and the angular momentum are transported along the poloidal field lines.

Finally, from eqs.(29,75) one obtains the following useful result

$$(B^2 - D^2)\alpha^2 = B^2(\alpha^2 - \beta^2) \begin{array}{l} +(\boldsymbol{\omega}\cdot\boldsymbol{B} + \boldsymbol{\beta}\cdot\boldsymbol{B})^2 \\ -B^2\left(\omega^2 + 2\boldsymbol{\omega}\cdot\boldsymbol{\beta}\right). \end{array} \tag{84}$$

4 GENERALIZED OHM'S LAW

It is generally accepted that the magnetospheres of black holes are filled with perfectly conducting e^+-e^- plasma (Blandford & Znajek 1977; Phinney 1982; Beskin et al.1991; Hirotani & Okamoto 1998). Should, however, a current sheet be formed in the magnetosphere (see Komissarov, 2002) the perfect conductivity approximation would fail and a model of electric resistivity would be required. It is well known that magnetic field strongly effects the electric properties of plasma by suppressing electric conductivity across the magnetic field lines and, thus, making the simple scalar Ohm's law inadequate. In fact, the total electric current splits into three components

$$\boldsymbol{j} = \sigma_\parallel \check{\boldsymbol{E}}_\parallel + \sigma_\perp \check{\boldsymbol{E}}_\perp + \boldsymbol{j}_d, \tag{85}$$

where $\check{\boldsymbol{E}}_\parallel$ is the component of electric field parallel to the magnetic field, $\check{\boldsymbol{E}}_\perp$ is the component of electric field perpendicular to the magnetic field, and $\boldsymbol{j}_d$ is the drift current which is perpendicular both to the electric and to the magnetic field vectors (Cowling 1976; Mestel 1999). The magnetospheric plasma is collisionless and its resistivity arises via collective processes, "the anomalous resistivity", and emission of photons, "the radiative resistivity". The radiative resistivity associated with the inverse Compton scattering of the photons emitted by the accretion disc has already been considered as a source of the internal resistivity in the potential gaps of the black hole magnetospheres (Beskin et al.1991; Hirotani & Okamoto 1998). Since, this is a rather simple and yet robust mechanism, it deserves to be considered in details.

If the gyration and the collisional time-scales are much smaller compared to the macroscopic time-scale then the mean velocity of a charged particle in electromagnetic and radiation fields, as observed by the local FIDO, is governed by

$$q(\check{\boldsymbol{E}} + \boldsymbol{v}\times\check{\boldsymbol{B}}) - (W^2-1)\sigma_T u_b \frac{\boldsymbol{v}}{v} = 0, \tag{86}$$

where the last term describes the inverse Compton interaction with soft background photons (Beskin et al.1991; Hirotani & Okamoto 1998). Here $\boldsymbol{p}$, $\boldsymbol{v}$, W, and $q=\pm e$ are the momentum, the velocity, the Lorentz factor, and the electric charge of the particle respectively, σ_T is the Thomson cross section, and u_b is the energy density of the radiation field. For simplicity, we assume that the radiation field is isotropic (Since the Boyer-Lindquist FIDO becomes singular near the event horizon this condition cannot be satisfied there at any length. However, for the Kerr-Schild FIDO this seems to be more or less acceptable everywhere.) One can solve this equation for the perpendicular and the parallel to the magnetic field components of velocity to obtain

$$\boldsymbol{v}_\parallel = \pm\frac{e}{\chi}\check{\boldsymbol{E}}_\parallel, \tag{87}$$

$$\boldsymbol{v}_\perp = \pm\frac{e}{\chi}\frac{1}{1+\delta^2}\check{\boldsymbol{E}}_\perp + \frac{\delta^2}{1+\delta^2}\frac{\check{\boldsymbol{E}}\times\check{\boldsymbol{B}}}{\check{B}^2}, \tag{88}$$

where

$$\chi = mW\nu_c, \tag{89}$$

$$\delta = \nu_b/\nu_c, \tag{90}$$

where

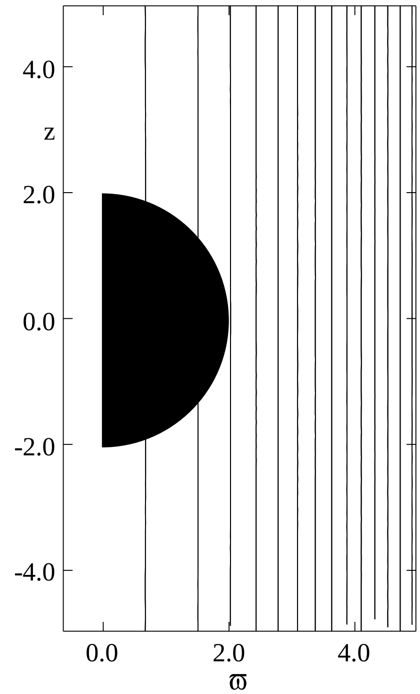

Figure 1. Schwarzschild black hole in uniform magnetic field. The black circle shows the position of the event horizon and the continuous lines show the magnetic flux surfaces.

$$\nu_b = \frac{e\check{B}}{mWc} \tag{91}$$

is the electron gyration frequency,

$$\nu_c = \frac{(W^2-1)\sigma_T u_b}{mWv} \tag{92}$$

is the effective frequency of the inverse Compton collisions; here m is the particle rest mass. The last term in eq.(88) does not depend on the sign of the electric charge and describes the usual drift motion effected by the collisions.

Equations (87,88) give us the generalized Ohm law of the same form as eq.(85) with

$$\sigma_\parallel = \frac{ne^2}{mW\nu_c} \tag{93}$$

$$\sigma_\perp = \frac{1}{1+\delta^2}\sigma_\parallel \tag{94}$$

$$\boldsymbol{j}_d = \rho\frac{\delta^2}{1+\delta^2}\frac{\check{\boldsymbol{E}}\times\check{\boldsymbol{B}}}{\check{B}^2}, \tag{95}$$

and

$$\rho = e(n_+ - n_-), \quad n = n_+ + n_-, \tag{96}$$

where $n_\pm$ are the number densities of electrons and positrons.

The typical values of $\check{B}$ and u_b in vicinity of a supermassive black of $M \approx 10^8 M_\odot$ are $\check{B} \approx 10^4$Gauss and $u_b \approx 10^7 \mathrm{erg\,s^{-1}}$. Hence, we have

$$\nu_c \approx 0.1W, \mathrm{s}^{-1} \qquad \nu_b \approx 10^{11} W^{-1}\mathrm{s}^{-1},$$

and

$$\delta \approx 10^{12} W^{-2}, \tag{97}$$

where W is the typical Lorentz factor of charged particles. Thus, the conductivity across the magnetic field is strongly suppressed indeed, and the drift velocity is given by the familiar expression

$$\boldsymbol{v}_d = \check{\boldsymbol{E}} \times \check{\boldsymbol{B}} / \check{B}^2.$$

For the Goldreich-Julian number density, $n_{GJ} \approx 0.1\,\mathrm{cm}^{-3}$, we obtain

$$\sigma_\parallel = 10^8 W^{-2} \mathrm{s}^{-1} \qquad \sigma_\perp = 10^{-16} W^2 \mathrm{s}^{-1},$$

whereas the macroscopic frequency is

$$\nu_m = \frac{c^3}{2MG} \approx 10^{-3} \mathrm{s}^{-1}.$$

Thus, one may confidently put $\check{\boldsymbol{E}}_\parallel = 0$ and ignore the cross-field conductivity current, $\sigma_\perp \check{\boldsymbol{E}}_\perp = 0$. This corresponds to the limit of force-free electrodynamics. Indeed, under these conditions

$$\rho \check{\boldsymbol{E}} + \boldsymbol{j} \times \check{\boldsymbol{B}} = \rho \check{\boldsymbol{E}}_\perp + \boldsymbol{j}_d \times \check{\boldsymbol{B}} = 0.$$

In this limit, the role of the $\check{\boldsymbol{E}}_\perp$ component of electric field is reduced to driving of the drift current.

Inside a current sheet the cross-field conductivity can no longer be ignored. In fact, it has got to be governed by a self-regulatory mechanism ensuring marginal screening of the electric field. Indeed, let us assume, for a moment, that the unscreened component of electric field is of the same order as the magnetic field. Then from equation (86) it follows that

$$W \approx \sqrt{\frac{e\check{B}}{\sigma_T u_b}} \approx 10^6. \tag{98}$$

This implies $\delta \approx 1$ (see eq.97) and, thus, similar conductivities both along and across the magnetic field. However, particles with such a high Lorentz factor are bound to launch copious pair cascades (Beskin et al.1991; Hirotani & Okamoto 1998). This would dramatically increase the electric conductivity and lead to effective reduction of the unscreened component of the electric field. Thus, the electromagnetic field of a magnetospheric current sheet is expected to be very close to the state of marginal screening with

$$\check{B}^2 - \check{E}^2 = 0. \tag{99}$$

(In fact, the electric field should remain slightly stronger than the magnetic field.) Since in this state, the typical particle's Lorentz factor is much smaller than the one given by eq.(98), one should have

$$\sigma_\parallel \gg \sigma_\perp, \quad \check{E}_\perp \gg \check{E}_\parallel,$$

and

$$\boldsymbol{j}_d = \rho \frac{\check{\boldsymbol{E}} \times \check{\boldsymbol{B}}}{\check{B}^2}. \tag{100}$$

Summarizing, the cross-field conductivity is essentially zero in the main body of the black hole magnetosphere, where it is basically force-free, and dramatically increases in current sheets to ensure that the magnitude of $\check{\boldsymbol{E}}_\perp$ exceeds the magnitude of the magnetic field only by a small margin.

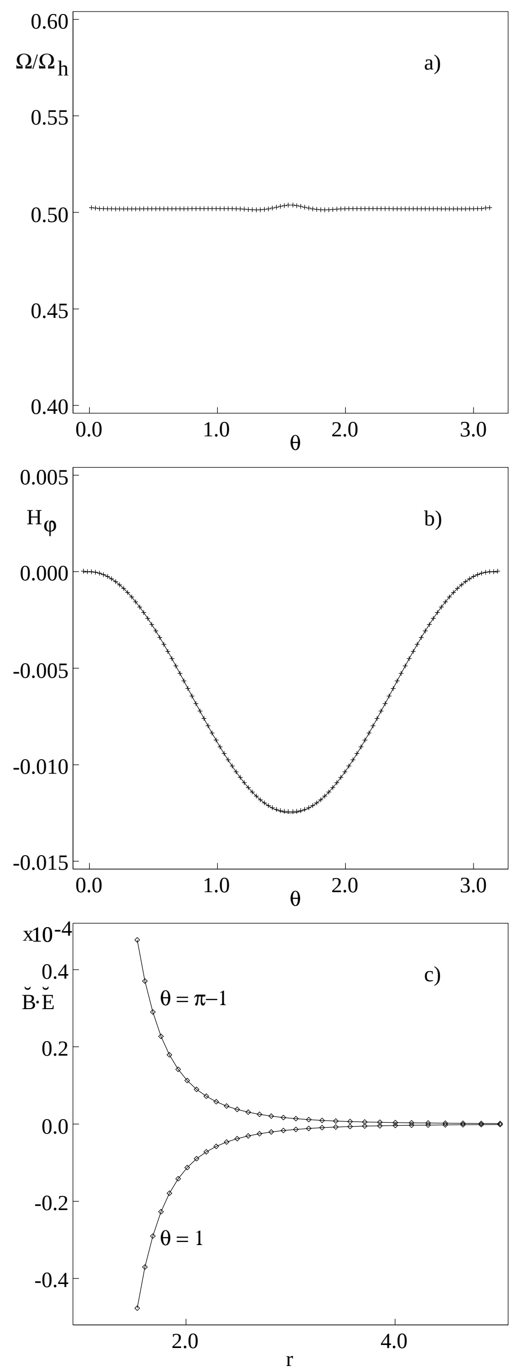

Figure 2. Monopole field solution for $a = 0.1$ and $B_0 = 1$ at time $t = 50$. Panel a) shows the angular velocity of magnetic field lines at r=3. The perturbative solution of Blandford and Znajek gives $\Omega = 0.5\Omega_h$, where Ω_h is the angular velocity of the black hole. Panel b) shows H_ϕ of the numerical solution (the crosses) and of the perturbative solution (the continuous line) at $r = 3$. Panel c) shows $\check{\boldsymbol{E}} \cdot \check{\boldsymbol{B}}$ along $\theta = 1$ and $\theta = \pi - 1$. The small unscreened component $\check{\boldsymbol{E}}_\parallel$ of electric field drives the conductivity current towards the black hole in the upper hemisphere and away from it in the lower hemisphere.

5 NUMERICAL STUDY OF BLACK HOLE MAGNETOSPHERES

To describe the black hole space-time we adopted the Kerr-Schild coordinates, $\{t, \phi, r, \theta\}$, which are free from the coordinate singularity at the event horizon hampering the Boyer-Lindquist coordinates (see Appendix B). This allows us to put the inner boundary of the computational domain inside the horizon and impose radiative boundary conditions on this boundary.

All simulations described below are axisymmetric. The computational grid is uniform in the θ-direction with $\Delta\theta = \pi/n_\theta$, where n_θ is the total number of cells in this directions. The cell size in the r-direction, Δr, is determined via the condition of the same length in both directions, $\gamma_{rr}\Delta r^2 = \gamma_{\theta\theta}\Delta\theta^2$. The time step is determined by the Currant stability condition.

The details of the resistivity model used in these simulations are given in Appendix C3.

5.1 Wald's solution

Wald (1974) obtained the following vacuum solution for a rotating black hole immersed into a uniform magnetic field aligned with hole's rotational axis:

$$F_{\mu\nu} = B_0(m_{[\mu,\nu]} + 2ak_{[\mu,\nu]}), \tag{101}$$

where $k^\nu = \partial_t$ and $m^\nu = \partial_\phi$ are the Killing vectors of the Kerr spacetime.

In the case of a Schwarzschild black hole eq.(101) reads

$$\boldsymbol{E} = 0, \qquad \boldsymbol{B} = \frac{B_0}{2\sqrt{\gamma}}\left(0, -\gamma_{\phi\phi,\theta}, \gamma_{\phi\phi,r}\right). \tag{102}$$

Outside of the horizon this solution satisfies the plasma equations (14-17,85) with zero ρ and $\boldsymbol{j}$. Indeed, from eq.(29) one finds

$$\boldsymbol{D} = -\frac{1}{\alpha}\boldsymbol{\beta}\times\boldsymbol{B}.$$

Thus, $\boldsymbol{D}_\parallel = 0$ and no electric current is driven along the magnetic field. Provided $B^2 - D^2 > 0$ no electric current will be driven across the magnetic field lines either. From eq.(84) one has

$$B^2 - D^2 = B^2\left(\frac{\alpha^2 - \beta^2}{\alpha^2}\right) + \left(\frac{\beta\gamma_{rr}B^r}{\alpha}\right)^2$$

which is strictly positive outside of the event horizon. (Inside of the horizon $\alpha^2 - \beta^2 < 0$ and $B^2 - D^2$ becomes negative near the equatorial plane where $B^r = 0$. However, these details do not effect the exterior solution.)

The computational grid in this test problem has 100 cells in the θ-direction and 80 cells in the r-direction covering the domain $r \in [1.4, 29]$. The initial solution is described by eq.(102). Figure 1 shows the magnetic flux surfaces of the numerical solution at time $t = 5$ as well as the flux surfaces of the exact steady-state solution (102). In fact, these solutions are so close that one cannot see the difference between them in this figure.

5.2 Blandford-Znajek's monopole solution.

Using a perturbation method Blandford and Znajek(1977) constructed a perturbative analytic solution for a slowly rotating black hole with monopole magnetic field that matches the flat space solution of Michel(1973) at infinity and satisfies Znajek's "boundary condition" (see Sec. 6.2) imposed at the event horizon. The zero order solution is the one for a nonrotating black hole with purely radial magnetic field

$$B^r = B_0 \sin\theta/\sqrt{\gamma}. \tag{103}$$

If $a \ll 1$ then the poloidal magnetic field is not expected to be very different from purely radial with B^r given by (103) and, thus, $B^r\sqrt{\gamma}$ remains constant along the field line. Moreover, the Znajek condition (eq.118) reads

$$H_\phi = (\Omega - \Omega_h)\sin\theta B^r\sqrt{\gamma}, \tag{104}$$

where $\Omega_h = a/(r_+^2 + a^2) \approx a/4$ is the angular velocity of the black hole. On the other hand, Michel's monopole solution in flat spacetime gives

$$H_\phi = -\Omega\sin\theta B^r\sqrt{\gamma}. \tag{105}$$

Matching of H_ϕ given by (104) with H_ϕ given by (104) leads to

$$\Omega = 0.5\Omega_h = a/8 \quad \text{and} \quad H_\phi = -\frac{aB_0}{8}\sin^2\theta \tag{106}$$

In these simulations case we used $B_0 = 1$ and put $a = 0.1$ because for this value of a the corresponding force-free numerical solution is known to be very close to the perturbative one (Komissarov 2001b). The computational grid in this test problem had 100 cells in the θ-direction and 150 cells in the r-direction covering the domain $r \in [1.4, 260]$. We tried two very different initial solutions for this problem. One of them describes the vacuum monopole field (this solution was found numerically.) The other one has the same $\boldsymbol{B}_p$ as in the Blandford-Znajek solution and $\boldsymbol{E} = 0$. However, in both these cases the outcome was the same, the numerical solution gradually evolved towards the Blandford-Znajek one. Figure 2 shows the angular distribution of Ω and H_ϕ at $r = 3$ as well as the distribution of the parallel component of the electric field in the northern and in the southern hemi-spheres at $t = 50$.

5.3 Split-monopole solution

Since the magnetic charges do not seem to exist, the monopole solution of Blandford and Znajek (1977) is rather artificial. A small modification, namely alternation of the magnetic field direction in one of the hemi-spheres, seems to overcome this problem. The result, known as the "split-monopole" solution, is still a force-free solution but now with zero total magnetic flux. However, such a configuration is meaningful only if there is a massive perfectly conducting thin disc in the equatorial plane of the black hole. Otherwise, the equatorial current sheet is not sustainable – the magnetic field is expected to reconnect and "fly away". Indeed, this is what is observed in numerical simulations (see Figure 3.) In this problem $a = 0.1$ and we use almost the same grid as in the Wald problem (Sec.5.1).

5.4 The Magnetospheric Wald Problem for rotating black holes

The Blandford-Znajek solution is the only global analytical solution for magnetospheres of rotating black holes found

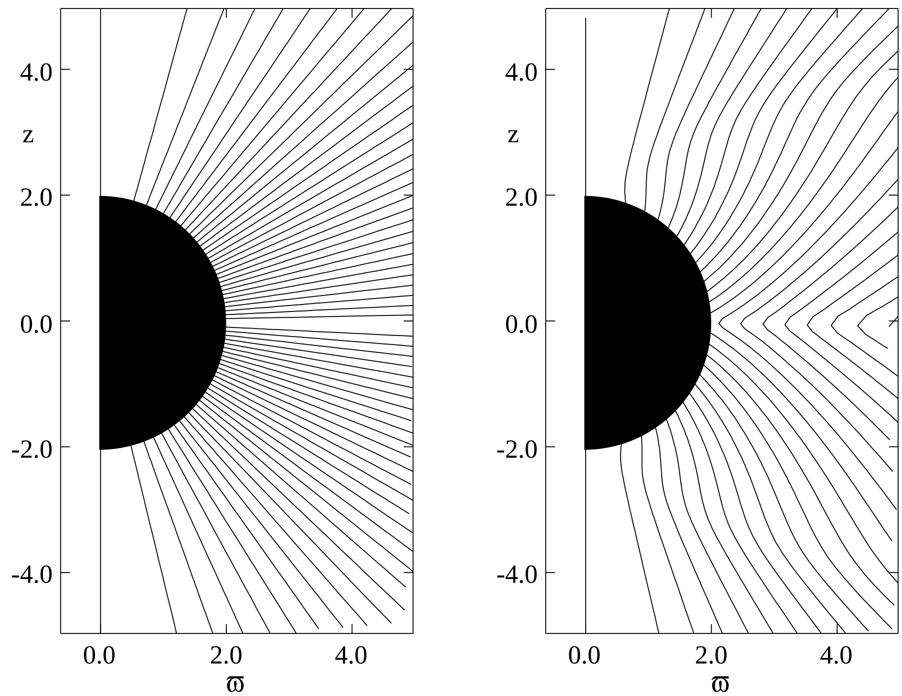

Figure 3. Escape of the split-monopole magnetic field from a Schwarzschild black hole. *Left panel:* Magnetic flux surfaces of the split-monopole solution which was used as an initial solution in these numerical simulations. *Right panel:* Magnetic flux surfaces of the numerical solution at $t = 5$.

so far and for this reason it has been playing a key role in the development of the black hole electrodynamics. One important property of this solution is that all magnetic field lines penetrate the black hole horizon. Macdonald (1984) attempted to construct numerical steady-state solutions for a more reasonable configuration of magnetic field where only a fraction of magnetic field lines originates from the black hole itself. The remaining magnetic flux splits between the field lines originating from the accretion disk and the field lines passing through the gap between the hole and the disc. In general, the angular velocity of magnetic field lines in steady-state force-free magnetospheres has to be prescribed, so one faces the task of setting physically sensible boundary conditions for all these three different types of magnetic field lines. In the case of the field lines originating from the accretion disc the solution is obvious. Their angular velocity is given by the angular velocity of the disc at the foot points. As for the other two kinds of magnetic field lines, this task is less trivial. In their solution, Macdonald and Thorne(1982) and later Macdonald(1984) appealed to the existing analogy between the black hole horizon and a rotating conducting sphere. They concluded that only the field lines penetrating the event horizon rotate, whereas in the gap $\Omega = 0$.

A somewhat simpler problem is the magnetospheric (plasma-filled) version of the Wald (1974) problem for a rotating black hole (see also Sec.5.1). In this problem, just like in the problem considered by Macdonald (1984), only a small fraction of magnetic field lines penetrate the black hole horizon. If the analysis of Macdonald & Thorne (1982) was correct then only these field lines would be forced to rotate. Komissarov(2002b) tried to find a steady state force-free solution to this problem by means of time-dependent numerical simulations but failed. The numerical solution invariably evolved towards the state where $B^2 - D^2$ turned negative inside the ergosphere. In fact, the solution seemed to indicate the development of a current sheet in the equatorial plane within the ergosphere with all magnetic field lines penetrating the current sheet being forced to rotate in the same sense as the black hole. If this conclusion is correct, a critical revision of the current perception of the role of the event horizon in the black hole electrodynamics, as well as of the virtues of the Membrane Paradigm, is required. Thus, the magnetospheric Wald problem is an ultimate Rosetta Stone for the research into the black hole electrodynamics.

To achieve high resolution within the ergosphere these simulations were carried out using the multi-grid technique. We start with a relatively low resolution grid and continue simulations until the solution becomes more or less steady within $r = 4$. Then the resolution is increased by the factor of 2 and the simulations are continued until new approximately steady-state solution is reached and so on. During the grid refinement the numerical solution on the finer grid is found via interpolation. The final grid has 800 cells in the θ-direction ($\theta \in [0, \pi]$) and 1000 cells in the r-direction ($r \in [0.9r_+, 110]$). The initial solution is described by the same $\boldsymbol{B}$ as in the vacuum solution of Wald (1974, eq.101) and has $\boldsymbol{E} = 0$, which implies a non-rotating magnetosphere.

Figure 4 shows the final solution, at $t = 126$, for a

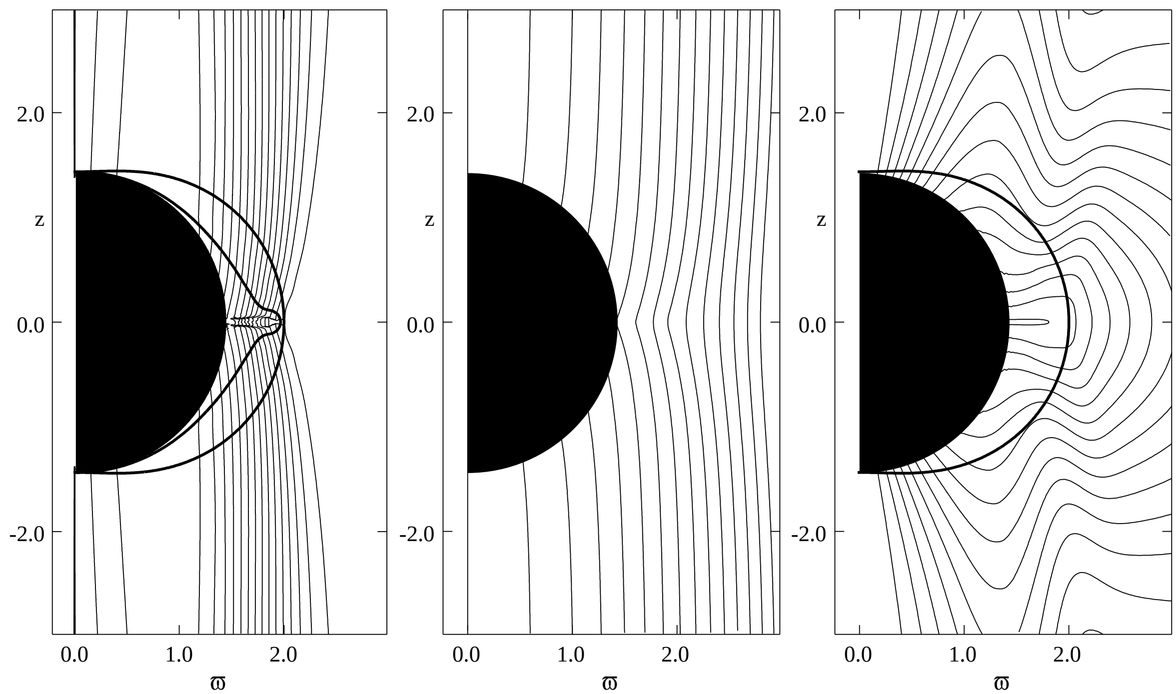

Figure 4. Magnetospheric Wald problem. *Left panel:* The angular velocity of magnetic field lines. There are 15 contours equally spaced between 0 and 0.67. The angular velocity first gradually increased towards the axis but then reaches a maximum and goes slightly down. The thick lines show the ergosphere (the outer line) and the inner light surface (the inner line). *Middle panel:* The magnetic flux surfaces. *Right panel:* The distribution of $(B^2-D^2)/\max(B^2,D^2)$. There are 15 contour equally spaced between -0.12 and 1.0. This quantity monotonically decreases towards the current sheet in the equatorial plane within the ergosphere. The thick line shows the ergosphere.

Kerr black hole with $a=0.9$. As suggested in Komissarov(2002b), a current sheet is formed in the equatorial plane within the black hole ergosphere. This is clearly seen in the right panel of fig.4 which shows the distribution of $(B^2-D^2)/\max(B^2,D^2)$. Near the equator the predominantly radial electric field is larger than the magnetic field and drives the electric current across the poloidal magnetic field lines. Both the radial component (the middle panel of fig.4) of magnetic field and its azimuthal component exhibit a break in the equatorial plane on the scale of the current sheet. The most important result is shown in the left panel of fig.4: all magnetic field lines penetrating the ergosphere are forced into rotation in the same sense as the black hole irrespective of whether they eventually cross the event horizon or not. Along these field lines there are outgoing fluxes of both energy and angular momentum. Indeed, in steady state force-free magnetospheres the angular momentum flux is proportional to H_ϕ and the energy flux is proportional to ΩH_ϕ (see eqs.82,83. Notice that Ω and H_ϕ are the same in the Boyer-Lindquist as in the Kerr-Schild coordinates; see Appendix B). As one can see in fig.5, both these quantities are nonvanishing along the field lines penetrating the ergosphere. Within the current sheet the electromagnetic energy and angular momentum are not conserved and, thus, the numerical results suggest that it is the current sheet that supplies both the energy and the angular momentum for the force-free magnetosphere above and below the sheet.

To show that this makes sense let us consider the sources of energy and angular momentum in the symmetry plane, $\theta=\pi/2$. Because of the symmetry $D_\parallel$ vanishes in this plane. Thus, we can ignore the dissipation due to $\sigma_\parallel$, and we can still introduce vector $\boldsymbol{\omega}$ to describe $\boldsymbol{D}$ as in eq.(76). In addition, the marginal screening of electric field implies $B^2=D^2$. The source terms in the Boyer-Lindquist coordinates have the same sign as in the Kerr-Schild coordinates and this allows us to utilize the Boyer-Lindquist coordinates to simplify calculations.

The source term in the energy equation (50) is

$$\mathcal{W}_t = -\boldsymbol{E}\cdot\boldsymbol{J}.$$

Substituting the expressions for $\boldsymbol{E}$ and $\boldsymbol{J}$ from (29,62,85) into this equation one obtains

$$\mathcal{W}_t = -\alpha^2\sigma_\perp D^2 - \alpha\sigma_\perp \boldsymbol{D}\cdot(\boldsymbol{\beta}\times\boldsymbol{B}).$$

Then, provided $\Omega<\Omega_z$, where $\Omega_z=-g_{\phi t}/g_{\phi\phi}$ is the angular velocity of the "zero angular momentum observer" (ZAMO, Bardeen et al.,1973), we have

$$\boldsymbol{D}\cdot(\boldsymbol{\beta}\times\boldsymbol{B}) = -|\boldsymbol{\beta}|B^2.$$

Hence, we obtain

$$\mathcal{W}_t = \alpha\sigma_\perp B^2(|\boldsymbol{\beta}|-\alpha). \qquad (107)$$

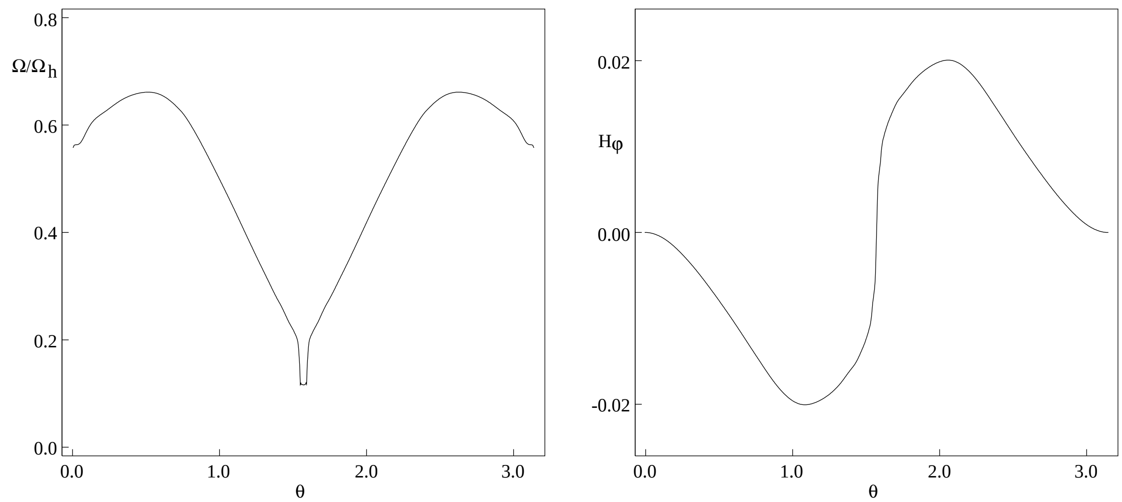

Figure 5. The distribution of the angular velocity of magnetic lines (*left panel*) and H_ϕ (*right panel*) in the magnetospheric Wald problem at $r = 1.8$.

Similar calculations lead to the expression for the angular momentum source, $\mathcal{W}_\phi$, in the equatorial plane

$$\mathcal{W}_\phi = -(\boldsymbol{J}\times\boldsymbol{B})\cdot\boldsymbol{m} = \alpha\sigma_\perp B^2. \tag{108}$$

Thus, provided the magnetosphere rotates slower then ZAMO, the resistive dissipation in the ergospheric current sheet can provide positive sources of electromagnetic energy and angular momentum. Since, the inner light surface encloses the current sheet (see the left panel of figure 4) the condition $\Omega < \Omega_z$ is satisfied in our numerical solutions. Obviously, this source of electromagnetic energy and momentum implies the existence of the same magnitude sink of energy and angular momentum for the radiation field. Thus, the energy transfer has to be essentially the same as proposed in (Punsly 2001). Namely, the electromagnetic field pushes plasma particles into orbits with negative energy at infinity, these particles push background photons into orbits with negative energy at infinity and finally these photons are swallowed by the black hole.

As the grid resolution increases the current sheet begins to show sings of unsteady behavior. Whether this is only a numerical effect or an indication of the current sheets instability remains to be investigated.

6 DISCUSSION. THE NATURE OF BLANDFORD-ZNAJEK MECHANISM

The results of numerical simulations presented in Sec.5 allow us to draw the following two general conclusions concerning the electrodynamics of black hole magnetospheres.

First of all, the rotational energy of black holes can indeed be extracted electromagnetically. In particular, the Blandford and Znajek solution is certainly stable and, hence, does not clash with causality.

On the other hand, there is much more to the electrodynamics of black holes than it is proposed in the Membrane Paradigm and the analogy between a magnetized rotating conducting sphere and the black hole horizon is at least incomplete. In fact, closer inspection of the causality arguments due to Punsly and Coroniti shows that it is the Membrane Paradigm which is most directly under attack. The Blandford-Znajek solution itself is involved mainly because it is widely considered as inseparably linked with the paradigm.

6.1 The origin of torque

6.1.1 Gravitationally induced electric field.

It is well known that a black hole with zero total electric and magnetic charge cannot have its own magnetic field and, ultimately, any magnetic field penetrating the hole's ergosphere has to be supported by external currents. This fact alone makes black holes very different from magnetized stars like pulsars. Moreover, a steady state axisymmetric vacuum electromagnetic field cannot be used to extract energy and angular momentum of a rotating black hole. Indeed, the steady-state vacuum equations,

$$\boldsymbol{\nabla}\times\boldsymbol{H} = 0, \quad \boldsymbol{\nabla}\times\boldsymbol{E} = 0,$$

ensure

$$H_\phi = E_\phi = 0 \tag{109}$$

for axisymmetric configurations. Then from eqs.(54,55) one finds that the poloidal components of the energy and the angular momentum flux vectors vanish as well. In order to extract energy and angular momentum the electromagnetic field has to be modified by magnetospheric charges and currents. However, in order to drive such currents and, perhaps, even to create charged particles via pair cascade in the first place (Blandford & Znajek 1977; Beskin et al.1991), the electric field should not be screened. That is at least one of the conditions (70,72) has to broken in the vacuum solution. As it is well known, the vacuum solution due to Wald (1974) has this property but we need to know whether it is generic.

Theorem. *There are no steady-state axisymmetric vacuum solutions supported by remote sources of magnetic field*

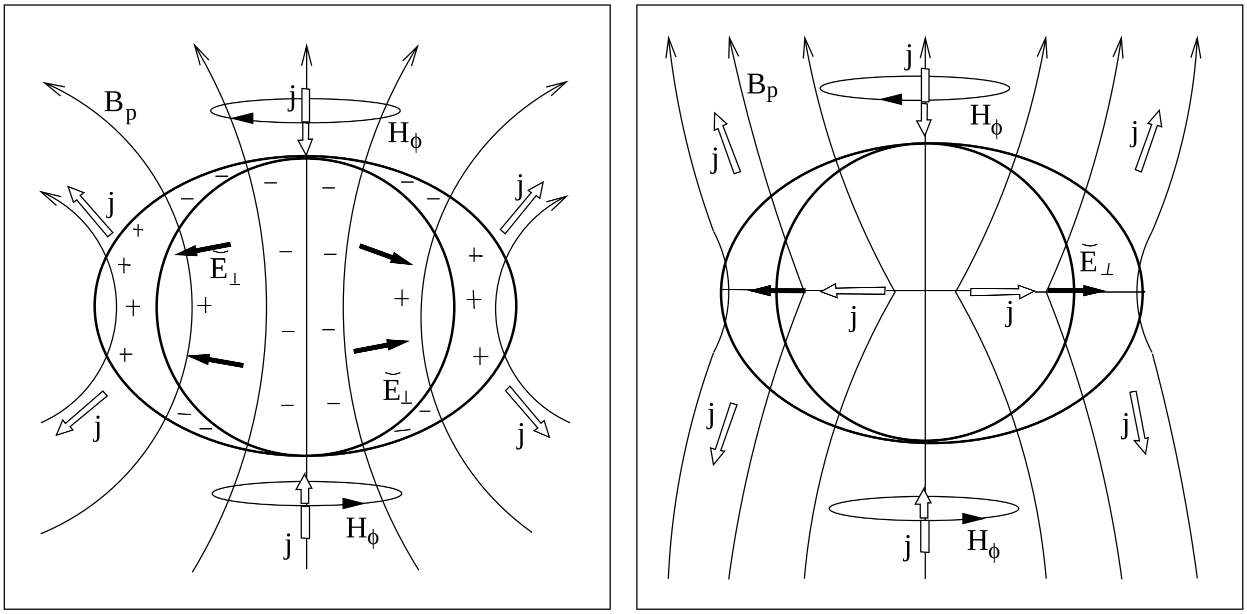

Figure 6. *Left panel:* The initial currents driven by the gravitationally induced electric field within the ergosphere as it is being filled with pair plasma during the thought experiment described in Sec.6.1.1. *Right panel:* The electric current system of the steady-state Wald's magnetosphere.

that simultaneously satisfy both

$$\boldsymbol{D}\cdot\boldsymbol{B} = 0 \quad \textit{and} \quad B^2 - D^2 > 0$$

along the magnetic field lines penetrating the ergosphere of a rotating black hole.

To prove this statement let us assume that electric currents of these sources can be arranged in such a way that $\boldsymbol{D}\cdot\boldsymbol{B} = 0$ everywhere in the vacuum zone surrounding the black hole. Just like in the case of a force-free magnetosphere this condition ensures the existence of the vector field $\boldsymbol{\omega} = \Omega\boldsymbol{m}$ such that Ω is constant the along magnetic field lines and

$$\boldsymbol{E} = -\boldsymbol{\omega}\times\boldsymbol{B}.$$

The remote sources may be regarded as non-rotating relative to the black hole and, thus, $\boldsymbol{E} = 0$ along the field lines penetrating the ergosphere. Then from eq.(29) one obtains

$$\boldsymbol{D} = -\frac{1}{\alpha}\boldsymbol{\beta}\times\boldsymbol{B}. \tag{110}$$

Thus, even though there are no external sources of electric field, the electric field is generated near the black hole as the result of the inertial frame dragging effect manifested in the shift vector $\boldsymbol{\beta}$. This is not entirely unexpected. Relative to any physical observer located within the ergosphere, including FIDO, these external sources do rotate. In the Boyer-Lindquist coordinates $\boldsymbol{\beta}$ is a purely azimuthal vector and $B_\phi = H_\phi/\alpha = 0$ (see eq.109). This allows to find

$$B^2 - D^2 = \frac{\alpha^2 - \beta^2}{\alpha^2} B^2. \tag{111}$$

Within the ergosphere $\alpha^2 - \beta^2 < 0$ and, hence, $B^2 - D^2 < 0$. Thus, no matter how strong is the magnetic field within the ergosphere, the gravitationally induced electric field is always stronger. This completes the proof.

Obviously, these external sources may not be infinitely far away and strictly non-rotating. In such a case, Ω is not exactly zero and instead of eq.(111) one obtains

$$\alpha^2(B^2 - D^2) = -B^2 f(\Omega, r, \theta), \tag{112}$$

where

$$f(\Omega, r, \theta) = g_{\phi\phi}\Omega^2 + 2g_{t\phi}\Omega + g_{tt}$$

is the light surface function (see Appendix A). Thus, the condition $B^2 - D^2 > 0$ is equivalent to the condition $\Omega > \Omega_{min}$ (see eq.A9). Since within the ergosphere $\Omega_{min} > 0$ and reaches the value of Ω_h at the event horizon, this requires the remote sources to rotate really fast. In fact, unless the remote sources of magnetic field are located within the outer light surface corresponding to Ω_{min}, which may be theoretically possible but which is highly unlikely to occur naturally, this condition cannot be satisfied.

Thus, the vacuum field created within a black ergosphere by distant sources must have unscreened electric field capable of driving electric currents, provided the charged particles are injected there somehow. The most popular mechanism involves an e^--e^+ pair cascade in strong electric and radiation field (Blandford & Znajek 1977; Beskin et al.1991). Let us consider an initial vacuum solution of the kind discussed above, that is a solution with $\boldsymbol{D}\cdot\boldsymbol{B} = 0$ and $\Omega = 0$, and figure out what occurs when plasma is injected (In fact, our initial numerical solutions in the Bladford-Znajek problem and the magnetospheric Wald problem are of this type.)

First of all, FIDO's electric field $\check{\boldsymbol{E}} = \boldsymbol{D}$ given by (110) will drive the conductivity current across the magnetic field lines within the ergosphere. This will result in the electric charge separation and the drop of the electrostatic potential along the magnetic field lines entering the ergosphere (see

figure 6). The induced parallel component of the electric field will drive the conductivity current along the magnetic field lines leading to the dynamo of H_ϕ according to the Ampere law $\boldsymbol{\nabla}\times\boldsymbol{H} = \boldsymbol{J}$. As one can see in the left panel of figure 6, the sign of the generated H_ϕ is exactly the one which is required to slow down the black hole. However, we need to verify that this is not a temporary phenomenon and a nonvanishing H_ϕ, and, hence, a nonvanishing poloidal current, will be a property of the magnetosphere when it relaxes to a steady-state.

6.1.2 *Poloidal currents in static magnetospheres.*

Let us suppose that the magnetic field lines penetrating the ergosphere are anchored to distant plasma of infinitely large inertia. Then the created magnetosphere will eventually become static with $\Omega = 0$, $\boldsymbol{E} = 0$. From eq.(84) one finds that in a force-free region of such magnetosphere

$$B^2 - D^2 = B^2\frac{\alpha^2-\beta^2}{\alpha^2} + \frac{1}{\alpha^2}(\boldsymbol{\beta}\cdot\boldsymbol{B})^2. \tag{113}$$

In the Boyer-Lindquist coordinates this reads

$$\alpha^2(B^2-D^2) = B^2(\alpha^2-\beta^2) + \left(\frac{\beta^\phi}{\alpha}\right)^2 H_\phi^2. \tag{114}$$

The difference between this result and equation (111) is entirely due to the azimuthal magnetic field created by the poloidal electric current. According to equation (76), the growth of this component of magnetic field does not lead to the growth of $\boldsymbol{D}$.

A number of important conclusions can be drawn from this simple result.

- First of all, inside the ergosphere $\alpha^2 - \beta^2 < 0$ and for $B^2 - D^2$ to be positive H_ϕ must be nonvanishing. This shows that screening of electric field by the injected plasma within the ergosphere implies generation of poloidal electric currents. These currents give rise to a nonvanishing H_ϕ and, thus, to a nonvanishing flux of angular momentum. Zero angular velocity of the magnetosphere means zero Poynting flux from the hole (see eq.83). Thus, the total mass of the hole, M, remains constant but its irreducible mass, M_{irr}, grows due to the loss of angular momentum. One may compare this case with a shorted out Faraday disk where its rotational energy is being used only for Ohmic heating of the disc itself.
- Secondly, it makes no difference whether the magnetic field lines penetrate the event horizon or not, *the only factor that matters is whether they penetrate the ergosphere.* The analogy between the event horizon and the rotating conducting sphere emphasized in the Membrane Paradigm does not reveal this important fact and, therefore, proves to be of rather limited value.
- Finally, it explains the origin of the equatorial current sheet in the magnetospheric Wald problem. Indeed, the magnetosphere is symmetric relative to the equatorial plane, and for this reason alone H_ϕ must vanish in this plane. Thus, the $B^2 - D^2 > 0$ condition cannot be satisfied in the ergospheric part of the plane and the force-free approximation breaks down. As we have seen in Sec.5.4 , this current sheet serves as a localized source of angular momentum for the surrounding force-free magnetosphere. Moreover, it provides the required closure of the electric circuit at the black hole end (see the right panel of fig.6).

6.1.3 *Poloidal currents in rotating magnetospheres*

Since the assumption of infinite inertia of the surrounding plasma, made in Sec.6.1.2, is unrealistic and was made only for the sake of argument, the outgoing flux of angular momentum will inevitably result in rotation and, thus, extraction of the black hole energy as well. The equilibrium value of Ω depends of the details of the interaction. In our simulations, the black hole was surrounded by massless plasma and the equilibrium value of Ω was determined by the rate of deposition of energy and angular momentum in the surrounding space by means of propagating waves.

Even after reaching a force-free equilibrium the magnetospheric electric field does not become completely screened. Within the ergospheric current sheet, $\check{\boldsymbol{E}}_\perp$ always remains slightly stronger than the magnetic field and keeps driving the cross field conductivity currents, thus, sustaining the potential drop along the magnetic field lines entering the current sheet. In the force-free region itself it is the small residual component of $\check{\boldsymbol{E}}_\parallel$ that drives the poloidal conductivity currents (see fig.2c), just as it occurs in the wires connected to the Faraday disc.

It is also quite clear why the magnetic field lines remaining outside of the ergosphere along their entire length do not rotate. Although the vacuum Wald solution has an unscreened $\check{\boldsymbol{E}}_\parallel$ component of the electric field which can trigger pair production and drive poloidal currents for a while, the injected charges eventually redistribute along the field lines and screen $\check{\boldsymbol{E}}_\parallel$. Then, because $\check{\boldsymbol{E}}_\perp$ is too weak (see eq.114), even in the equatorial plane, to drive the cross field current, the poloidal currents die out completely. The force free conditions are met even when $H_\phi = 0$.

The spatial grids of both the Boyer-Lindquist and the Kerr-Schild coordinates, though stationary relative to distant inertial observers at rest relative to the black hole, rotate superluminally relative to any local physical observer located within the ergosphere. This property of black hole space-time is crucial in determining the properties of their magnetospheres. To illustrate the point let us consider a steady-state magnetosphere rotating with angular velocity Ω in flat space-time (we assume that some particle injection mechanism ensures plentiful supply of electrical charges required to screen the electric field.) Let us introduce a spherical grid rotating with the same angular velocity. The corresponding coordinate transformation

$$t = t',\ r = r', \phi = \phi' - \Omega t',\ \theta = \theta',$$

where the primed coordinates refer to the nonrotating grid, results in the metric form

$$ds^2 = (\beta^2-\alpha^2)dt^2 + 2\beta_\phi d\phi dt + dr^2 + r^2(\sin^2\theta d\phi^2 + d\theta^2) \tag{115}$$

where

$$\alpha = 1,\ \beta^2 = \Omega^2\sin^2\theta r^2,\ \beta_\phi = \Omega\sin^2\theta r^2.$$

We notice that this metric is rather similar to the Kerr metric as the surface $r\sin\theta = \varpi_c = 1/\Omega$ separates the inner region where the time coordinate is time-like from the outer

region where it is space-like (obviously, ϖ_c is the cylindrical radius of the light cylinder.) Relative to the rotating grid the magnetosphere is static and, thus, $\boldsymbol{E}=0$. Calculations similar to those leading to eq.(114) give us

$$B^2 - D^2 = B^2(1-(\varpi/\varpi_c)^2) + \Omega^2 H_\phi^2. \tag{116}$$

Thus, high conductivity ensures $H_\phi^{'} = H_\phi \neq 0$ outside of the light cylinder. The similarity with black hole magnetospheres is startling.

The result (116) serves another goal. It shows that H_ϕ must remain nonvanishing in rotating magnetospheres of black holes for any value of $\Omega \neq 0$.

6.1.4 Where is the unipolar inductor of a Kerr black hole?

In the case of the Faraday disc, which is a classical example of a unipolar inductor, electrons are forced to participate in the disc rotation via collisions with other disc particles. This provides the electromotive force, $q\boldsymbol{v}\times\boldsymbol{B}$, which results in electric charge separation and, hence, the voltage drop between the disc rim and its centre. When the disc is used as battery in a closed electric circuit the electromotive force continues to push electrons against the electric force and across the magnetic field lines. This is essential for sustaining the potential drop and for providing the current closure. Spinning magnetized cosmic objects like stars or accretion discs generate an electric field in the very much same way. Such a field is often described as *rotationally induced*.

Although, the Membrane paradigm invites to treat black holes in a similar fashion, in reality they are rather different. Both in the Blandford-Znajek solution and in our solution to the magnetospheric Wald problem there is no any massive conducting rotating object and, thus, no usual electromotive force driving electric current over its surface. In spite of this curious feature the potential drop across the magnetic field lines still exists and the electric currents still flow.

The answer to this paradox seems to reside in another peculiar property of rotating black holes - contrary to our everyday experience the electric charge separation in not the only way of creating stationary electric field in their vicinity. The vacuum solution found by Wald(1974) shows that such an electric field can be induced *gravitationally.* Thus, the usual electromotive force is not required at least for initial charging of the black hole "battery". Punsly and Coronity (1990a) argued that such electric field can not sustain stationary electric currents. Their first point is based on the change of sign of the parallel component of the electric field in the exact Wald solution. Indeed, this seems to be inconsistent with the electric current flowing along the poloidal magnetic field line in one particular direction. However, the electric field modified by the magnetospheric charges does not have to retain this property. In their second point, they argue that the mere fact of existence of any initial electric field does not matter very much. For example, a capacitor can drive only a transient electric current. Unless a battery is continuously recharged via the action of some electromotive force it cannot drive a stationary electric current. In other words, the initial transient currents can redistribute electric charge in the black hole magnetosphere in such a way that the electric field becomes completely screened and can no longer drive the electric currents. However, as we have shown above, such a final state is not possible within the black hole ergosphere. Black holes do not allow stationary solutions with screened electric field and vanishing poloidal electric currents.

Thus, the electrodynamics of rotating black holes is very different from electrodynamics of usual magnetic rotators and their batteries operate on other principles than the classical unipolar inductor. The key role played by the ergosphere in black hole electrodynamics allows us to call it the "driving force" of the Blandford-Znajek mechanism.

6.2 Causality arguments

Apart from the absence of the proper unipolar inductor Punsly and Coronity (Punsly & Coroniti 1990a; Punsly 2001) criticized the electromagnetic mechanism on the ground of causality principle. The key point of their criticism is concerned with the role of Znajek's horizon condition in the Blandford-Znajek solution (Blandford & Znajek 1977, Znajek 1977; see also Sec.5.2.) Since Blandford and Znajek employed the Boyer-Lindquist coordinate system, the horizon appears as a singular boundary of their spatial domain and the Znajek condition appears as a boundary condition. In fact, this perception of the Znajek's condition is fully accomodated in the Membrane paradigm, where this condition is used to endow the event horizon with the properties of rotating conducting surfaces, reintroducing the missing unipolar inductor in a somewhat ghostly form.

Punsly and Coroniti (1990a) convincingly argued that this analogy must be wrong. They pointed out that the BZ-solution describes not just an outgoing wind, as in the case of pulsar winds, but also an ingoing wind that passes though its own critical surfaces (see also Takahashi et al. 1990 and Appendix A.) As the result, the event horizon is causally disconnected from the outgoing wind and, thus, not suitable for imposing boundary conditions that would determine the properties of the outgoing wind. This made Punsly and Coroniti (1990a) to conclude that although the Blandford-Znajek solution may be a valid solution of steady-state equations it must be unstable and thus the time-dependent solution would never evolve towards it. However, the results of numerical simulation presented in (Komissarov 2001b) and in this paper show just the opposite – the Blandford-Znajek solution is, in fact, asymptotically stable and, hence, causal.

The answer to this controversy seems to be very simple. Znajek's horizon condition is not a boundary condition after all. Indeed, Znajek derived the horizon condition from a very natural requirement. Namely, the electromagnetic field at the event horizon had to be non-singular when measured by a local free-falling observer. However, in the limit of force-free electrodynamics, the event horizon coincides with the fast critical surface of the ingoing wind. This immediately follows from the fact that the fast wave of force-free electrodynamics propagates with the speed of light (Komissarov 2002a). All this suggests that Znajek's condition is in fact a regularity condition at the fast critical point of the ingoing wind, obtained by Znajek in a somewhat unconventional way.

There is an important difference between a boundary condition and a regularity condition. Boundary conditions

are set on the boundaries of computational domain and select particular solutions to both steady-state and time-dependent problems. Regularity conditions apply only to steady-state problems when one is looking for solutions passing smoothly through critical points, at which the steady-state equations change their type.

In the Kerr-Schild coordinates, where there in no coordinate singulatity at the horizon, the critical nature of the Znajek condition becomes very clear. Let us consider a steady state force-free solution smoothly passing through the event horizon. In such a solution the angular velocity of magnetic field, Ω, and H_ϕ are constant along the magnetic field lines. Following Weber & Davis(1967) we can use these constants in order to find the relationship between B^ϕ and B^r along a given magnetic field line. First, we eliminate $\boldsymbol{D}$ from eq.(30) using eq.(76) to obtain

$$\boldsymbol{H} = \alpha\boldsymbol{B} + \frac{1}{\alpha}\left[\boldsymbol{\omega}(\boldsymbol{\beta}\cdot\boldsymbol{B}) - \boldsymbol{B}(\boldsymbol{\beta}\cdot\boldsymbol{\omega} + \beta^2) + \boldsymbol{\beta}(\boldsymbol{\beta}\cdot\boldsymbol{B})\right].$$

From this equation we derive, after rather involved calculations, the following result:

$$B^\phi = \frac{\alpha H_\phi - B^r \sin^2\theta(2r\Omega - a)}{\Delta \sin^2\theta}. \tag{117}$$

The denominator of the right hand side of this equation vanishes at the event horizon, where $\Delta = 0$. For B^ϕ to remain finite the numerator has to vanish as well and we obtain

$$H_\phi = \frac{\sin^2\theta}{\alpha_+}(2r_+\Omega - a)B^r = \frac{(2r_+\Omega - a)\sin\theta}{r_+^2 + a^2\cos^2\theta}A_{\phi,\theta}, \tag{118}$$

which is exactly the Znajek condition (Notice that H_ϕ, A_ϕ, and Ω are the same in the Kerr-Schild coordinates as in the Boyer-Lindquist coordinates; see Appendix B) Thus, Znajek's "boundary condition" is indeed a regularity condition at the fast critical point of the ingoing wind. In MHD approximation, in the case where the particle inertia is not negligibly small, the fast surface is located outside of the event horizon and Znajek's horizon condition is no longer needed to determine the steady-state wind solution (Beskin & Kusnetsova 2000).

In time, the dispute over causality of the Blandford-Znajek solution, and causality of the electromagnetic mechanism as such, gradually evolved into a dispute over the role played by different waves in the development of the system of poloidal currents in black hole magnetospheres, e.g. (Blandford 1991; Punsly 1996; Punsly 2001; Blandford 2002). The origin of this slight change of subject resides in the fact that in the Membrane paradigm the inner boundary conditions are imposed not at the actual event horizon but at the so-called "stretched horizon", located just outside of the actual one (Thorne et al.1986). This allows communication between the stretched horizon and the outgoing wind by means of fast waves giving hope of salvaging the perception of the event horizon as a unipolar inductor of black holes (Blandford 1991; Blandford 2002). Punsly (1996; 2001) dismissed this idea showing that in order to provide the necessary adjustment of poloidal currents the stretched event horizon would have to communicate with the outgoing wind by means of Alfvén waves. However, this is not possible as the inner critical Alfvén surface in the Blandford-Znajek solution is located well outside of the stretched horizon.

The conclusion of Punsly (2001) on the crucial role of Alfvén waves in establishing the global current system seems to be correct in general. This is particularly easy to see in the limit of force-free electrodynamics. In this approximation the electric charge and the electric current density can only be changed by hyperbolic waves. The fast waves cannot do this as they have identical properties to linearly polarised waves of vacuum electrodynamics (Komissarov 2002a). The only other option is the Alfvén waves.

However, once we have seen that 1) the event horizon does not play the role of a unipolar inductor, 2) the Znajek's horizon condition is just the usual regularity condition, and 3) the key role in the electrodynamic mechanism is played by the black hole ergosphere, this dispute has to be somewhat redirected. What we need to verify is that the ergosphere is causally connected with the outgoing wind. In fact, as it is shown in Appendix A1, the inner Alfvén surface is always located inside the ergosphere, and our numerical simulations are fully consistent with this result (see fig.4, A1). All these allow us to conclude that there is no causality clash associated the electrodynamic mechanism in general and with the Blandford-Znajek solution in particular.

7 CONCLUSIONS

- The 3+1 equations of black hole electrodynamics can be written in more general and simpler form than the classical formulation of Thorne and Macdonald (Thorne & Macdonald 1982; Macdonald & Thorne 1982; Thorne et al.1986). Our equations are very similar to the classical equations of electrodynamics in matter and hold in any system of coordinates which delivers time-independent metric form, e.g. Kerr-Schild coordinates.
- The inertia of magnetospheric plasma is not an essential element in the mechanisms of extraction of rotational energy of black holes involving electromagnetic field. We have seen no indications of any major deficiency of the electrodynamic model which would suggest a need for the more complex MHD model, at least at the black hole end. The force-free approximation, however, may break down locally via formation of dissipative current sheets. We have constructed a simple model for radiative resistivity based on the inverse Compton scattering of background photons and used this model to show the development of the equatorial current sheet within the ergosphere of a black hole with a dipolar magnetic field. This current sheet supplies energy and angular momentum for the surrounding force-free magnetosphere.

Having said that, we need to stress that the role of particle inertial has not been considered in this paper and requires further investigation. For example, one would expect the inertial effects to become important in the remote part of the outgoing wind, like they seem to do in the winds from neutron stars, e.g. (Mestel 1999; Kennel & Coroniti 1984).

- The gravitationally induced electric field is the ultimate cause of the poloidal currents in the black hole magnetospheres. Within the ergosphere this field cannot be screened by any static distribution of electric charge. This makes a "magnetized" black hole very different from the classical unipolar inductor (or any other battery), where the potential difference between terminals is created and sustained by the electromotive force which first separates electric charges and then drives electric currents against the electric field.

In fact, within the ergospheric current sheet the cross-field current flows along the electric field but not against it. The special role played by the ergosphere allows us to call it the "driving force" of the Blandford-Znajek mechanism. Since the same applies to the otherwise rather different Penrose mechanism (Penrose 1969), this suggests that it is the existence of the ergosphere that makes possible energy extraction from a black hole in any form.

- The Blandford-Znajek solution in particular, and the electromagnetic mechanism of extraction of rotational energy of black holes in general, do not clash with causality. First of all, the Znajek horizon condition is not a boundary condition but a regularity condition at the fast critical point. This perfectly justifies its utilization in the Blandford-Znajek monopole solution. Secondly, the ergosphere is causally connected to the outgoing wind by means of both fast and Alfvén waves. This conclusion is strongly supported by numerical simulations that show that the Blandford-Znajek monopole solution is asymptotically stable.
- Our results fully agree with the conclusion of Punsly and Coroniti (Punsly & Coroniti 1990a; Punsly & Coroniti 1990b) and Beskin & Kuznetsova (2000) on the superficial nature of the interpretation of the event horizon as a unipolar inductor of black holes. The failure of the Membrane paradigm to predict the outflow of energy and angular momentum along all magnetic field lines penetrating the ergosphere has clearly exposed its limitations. Although the analogy with conducting sphere is based on mathematically sound grounds, it does not account for all important properties of black hole electrodynamics and does not reveal the true physical nature of the Blandford-Znajek mechanism.

8 ACKNOWLEDGMENTS

I thank Brian Punsly for the highly motivating discussion of the Blandford-Znajek mechanism over the Internet and Roger Blandford for his useful comments on this subject. I also acknowledge the limited support of this research from PPARC via "A rolling programme of theoretical astrophysics research in Leeds". Finally, I would like to thank the anonimous referee for useful suggestions concerning the notation in the 3+1 electrodynamics.

APPENDIX A: LIGHT SURFACES

The physical significance of the light surfaces in the black hole magnetospheres is well understood and indisputable. However, the author of this paper could not find any more or less complete and systematic description of their properties. This section is intended to fill the gap and to provide a convenient reference for the reader of the paper.

A1 Basic properties of light surfaces

Consider a point orbiting a Kerr black hole with angular velocity Ω. The type of its world line depends on the sign of the function

$$f(\Omega,r,\theta)=g_{\phi\phi}\Omega^2+2g_{t\phi}\Omega+g_{tt}. \tag{A1}$$

It will be time-like (subluminal rotation) if $f<0$, space-like (superluminal rotation) if $f>0$, and null if $f=0$. Similarly, a magnetosphere, rigidly rotating with angular velocity Ω, is divided into the regions of subluminal and superluminal rotation depending on the sign of $f(\Omega,r,\theta)$. The separating surfaces, defined via

$$f(\Omega,r,\theta)=0, \tag{A2}$$

are called "the light surfaces". Here we derive the basic properties of light surfaces of magnetospheres with $0<\Omega<\Omega_h$, where $\Omega_h=a/2r_+$ is the angular velocity of the black hole (without any loss of generality we assume that $a>0$.)

(i) *The light surfaces are symmetric relative to the equatorial plane.*

This property immediately follows from the symmetries of the metric tensor.

(ii) *There exist only two light surfaces, the inner one and the outer one. Inside of the inner surface and outside of the outer surface the rotation of the magnetosphere is superluminal.*

Consider the case $\Omega=0$. Then

$$f(\Omega,r,\theta)=g_{tt} \tag{A3}$$

and, thus, the only light surface is the ergosphere of the black hole. Because g_{tt} is positive inside of the ergosphere and negative outside of it, the rotation inside of this light surface is superluminal. Since $f(\Omega,r,\theta)$ is analytical, this light surface will continue to exist for $\Omega>0$, though its location may differ. We shell call it the "inner light surface". Since along the rotational axis eq.(A2) is reduced to $g_{tt}=0$ for any Ω, this surface always includes the point $(r,\theta)=(r_+,0)$.

If $0<\Omega\ll 1$ then another light surface emerges from infinity. Indeed, for $r\gg 1$

$$f(\Omega,r,\theta)=r^2\sin^2\theta\Omega^2-1 \tag{A4}$$

and, thus, eq.(A4) has the solution

$$r=\frac{1}{\Omega\sin\theta}, \tag{A5}$$

which moves to infinity as $\Omega\to 0$. We shell call this light surface the "outer light surface". From (A4) it follows that outside of this surface the magnetosphere rotates superluminally. Notice, that according to eq.(A4) no other light surface can continue to infinity for any value of Ω.

Since $f(\Omega,r,\theta)$ is analytical, an additional light surface can only 1) bifurcate from a point where $f(\Omega,r,\theta)$ has a local minimum or maximum, or 2) appear as a result of splitting of already existing light surfaces. To exclude the first option we notice that

$$\begin{aligned}\rho^4\partial f/\partial\theta = \quad & [(\Delta\rho^4+2r(a^2+r^2)^2)\Omega^2- \\ & -4ar(a^2+r^2)\Omega+2a^2r]\sin 2\theta,\end{aligned}$$

which is positive for $r>r_+$ with exceptions of the rotational axis and the equatorial plane where it vanishes. However, the only point of the rotational axis where $f(\Omega,r,\theta)$ ever vanishes belongs to the inner light surface. Similarly, there are only two locations on the equatorial plane where f ever vanishes and those belong to the inner and the outer light surfaces for all values of Ω. Indeed, along the equator $f=s(\Omega,r)/r$ where

$$s(\Omega, r) = (r^3 + a^2 r + 2a^2)\Omega^2 - 4a\Omega + 2 - r. \tag{A6}$$

Since s is a cubic polynomial in r, it has at most three roots. The extremes of the cubic are given by

$$r^2 = \frac{1}{3}\left(\frac{1}{\Omega^2} - a^2\right), \tag{A7}$$

which shows that one of the roots is always negative. For $\Omega \ll 1$ the two other roots are $r_{in} = 2$ and $r_{out} = 1/\Omega$. Obviously they belong to the inner and the outer light surfaces. This also proves that no additional light surfaces can appear via splitting of the inner or the outer ones.

Finally, on the event horizon

$$f(\Omega, r, \theta) = \frac{4r_+}{\rho_+^2}\sin^2\theta(\Omega - \Omega_h)^2, \tag{A8}$$

showing that no light surface can bifurcate from the event horizon either.

(iii) *Inside the inner light surface the rotation is "too slow" whereas outside of the outer light surface it is "too fast".*

The condition of subluminal rotation, $f(\Omega, r, \theta) < 0$, leads to the following constraint on Ω:

$$\Omega_{min} < \Omega < \Omega_{max}, \tag{A9}$$

where

$$\Omega_{min} = \Omega_z - \sqrt{\Omega_z - g_{tt}/g_{\phi\phi}},$$

$$\Omega_{max} = \Omega_z + \sqrt{\Omega_z - g_{tt}/g_{\phi\phi}},$$

where $\Omega_z = -g_{t\phi}/g_{\phi\phi}$ is the angular velocity of the local zero angular momentum observer (ZAMO). On the horizon $\Omega < \Omega_h = \Omega_{min}$ and by continuity $\Omega < \Omega_{min}$ in the whole of the inner superluminal region. Similarly, for $r \to \infty$ one has $\Omega_{max} < 1/r\sin\theta < \Omega$ and by continuity $\Omega > \Omega_{max}$ in the whole of the outer superluminal region.

(iv) *The inner and the outer light surfaces do never have common points.*

Since, as we have established above, $\partial f/\partial\theta > 0$ in the space between the rotational axis and the equatorial plane, all we need to show is that the root r_{in} of eq.(A6) is always less than the root r_{out}. We already know that this is true for $\Omega \ll 1$ and, hence, it is sufficient to show that these roots of eq.(A6) never merge. From eqs.(A6,A7) one finds the merger condition

$$\xi(a, \Omega) = (1 + a\Omega)^3 + 27a\Omega^3 - 27\Omega^2 = 0.$$

It is easy to see that $\partial\xi/\partial a > 0$. Moreover, direct calculations show that $\xi(a, \Omega_h(a)) \geq 0$, where the equality holds only if $a = 1$. These ensure $\xi(a, \Omega) > 0$ for $0 < \Omega < \Omega_h(a)$.

(v) *The inner light surface is located between the ergosphere and the event horizon.*

At the ergosphere

$$f(\Omega, r, \theta) = g_{\phi\phi}\Omega(\Omega - 2\Omega_z).$$

For $0 < \Omega \ll 1$ one has $\Omega < \Omega_z$ and $f < 0$. Thus, the inner light surface shifts inside the ergosphere as Ω turns positive. A light surface can also make contact with the ergosphere when $\Omega = 2\Omega_z$ but that can only be the outer light surface. Indeed, simple calculations show that $\partial\Omega_z/\partial r < 0$ for $r > r_+$. Thus, along the radial ray passing though the point of

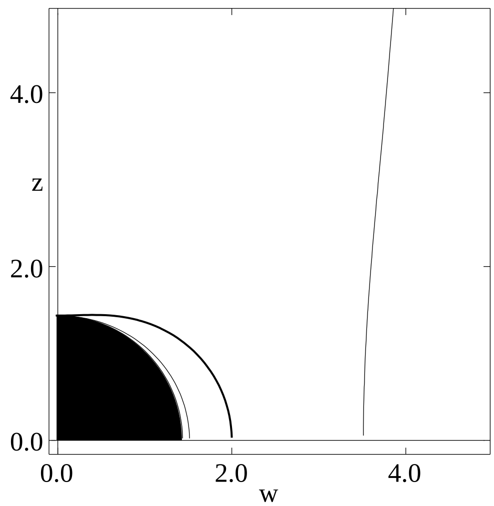

Figure A1. The light surfaces (thin lines) of a rigidly rotating magnetosphere. Here $\Omega = 0.7\Omega_h$ and $a = 0.9$. The thick line shows the ergosphere.

contact $f(\Omega, r, \theta)$ is positive all the way from the ergosphere to infinity.

The conclusion that the inner light surface always remains outside of the event horizon simply follows from eq.(A8).

(vi) *The coordinate r of the inner light surface monotonically increases with θ for $0 < \Theta < \pi/2$. For the outer light surface there holds exactly the opposite.*

Direct inspection of the lights surfaces found in the limit $\Omega \ll 1$ (see eq.A3 and eq.A5) immediately shows that they have this property. Thus, one need only to verify that $dr/d\theta$ does not vanish anywhere on the critical surfaces with the exceptions of the equatorial plane and the symmetry axis. Since

$$\frac{dr}{d\theta} = -\frac{\partial f}{\partial\theta}/\frac{\partial f}{\partial r}$$

this follows from the fact that $\partial f/\partial\theta$ does not vanish for $0 < \Theta < \pi/2$ (see the proof of property (ii)).

The geometrical properties of light surfaces are summarized in figure A1.

A2 Light surfaces and magnetically driven winds

Consider a force-free region of a steady-state magnetosphere. As we have established above, each magnetic field line that penetrates the black hole ergosphere is forced to rotate with angular velocity $0 < \Omega < \Omega_h$ and may cross the light surfaces corresponding to this value of Ω. Let us show that in the inner superluminal region charged particles are forced to move towards the black hole whereas in the outer superluminal region they are forced to move away from it. To simplify calculations we shell use the Boyer-Lindquist coordinates and assume, without any loss of generality, that the magnetic field line under consideration is outgoing ($B^r > 0$).

Any such particle slides freely along the magnetic field

line and participates in the drift motion across the field line. Thus, its velocity vector is

$$\boldsymbol{v} = \boldsymbol{D}\times\boldsymbol{B}/B^2 + \kappa\boldsymbol{B}, \tag{A10}$$

(for simplicity sake we ignore particle's gyration.) The radial component of $\boldsymbol{v}$ is limited from above and from below via the condition $v^2 < 1$. In the limit $v^2 = 1$ one has $\boldsymbol{v} = \boldsymbol{v}_\pm$, where

$$\boldsymbol{v}_\pm = \frac{1}{B^2}(\boldsymbol{D}\times\boldsymbol{B} \pm \boldsymbol{B}\sqrt{B^2 - D^2}). \tag{A11}$$

Using eqs.(29,75) to express $B^2 - D^2$ and $\boldsymbol{D}\times\boldsymbol{B}$ in terms of $\boldsymbol{B}$ and Ω one obtains the following result for the poloidal component of $\boldsymbol{v}$:

$$\boldsymbol{v}_{p\pm} = \eta_\pm \boldsymbol{B}_p, \tag{A12}$$

where

$$\eta_\pm = \frac{1}{B^2}\left(-l \pm \sqrt{l^2 - \frac{B^2}{\alpha^2} f(\Omega, r, \theta)}\right),$$

$$l = \frac{(\Omega - \Omega_z)H_\phi}{\alpha^2}.$$

Given the assumed direction of $\boldsymbol{B}_p$, $\boldsymbol{v}_{p+}$ has the highest possible and $\boldsymbol{v}_{p-}$ has the lowest possible radial component.

Since in the interior of the inner light surface $\Omega < \Omega_z$ and $f > 0$ we conclude that η_+ is negative there (notice that $H_\phi < 0$) and, thus, charged particles are bound to slide towards the black hole. As the result, no magnetic field line within the inner light surface can turn away from the black hole unless this takes place in the region where the force-free approximation breakes down (e.g. within the equatorial current sheet of the magnetospheric Wald problem, see figure 4.)

Similarly, one finds that in the outer superluminal region η_- is positive and, thus, charged particles are forced to slide away from the hole (Basically the same analysis was used by Goldreich & Julian (1969) with application to pulsar winds.)

A3 Light surfaces and Alfvén critical surfaces

The normal wavespeeds of Alfvén waves in force-free electrodynamics in FIDO's frame are given by

$$\mu_\pm = \boldsymbol{\mu}_\pm \cdot \boldsymbol{n} \tag{A13}$$

where

$$\boldsymbol{\mu}_\pm = \left(\boldsymbol{D}\times\boldsymbol{B} \pm \boldsymbol{B}\sqrt{B^2 - D^2}\right)/B^2 \tag{A14}$$

(Komissarov 2002a). By definition, at a critical Alfvén surface with the outgoing unit normal $\boldsymbol{n}$ either μ_+ or μ_- changes its sign. As $\boldsymbol{\mu}_\pm$ are given by exactly the same expressions as $\boldsymbol{v}_\pm$ (A11) we immediately obtain that

$$\mu_\pm = (\boldsymbol{n}\cdot\boldsymbol{B}_p)\eta_\pm. \tag{A15}$$

Thus, in the force-free limit the Alfvén surfaces coincide with the light surfaces. If $\boldsymbol{B}_p$ is outgoing then μ_+ corresponds to the outgoing wave and vanishes at the inner light surface. Inside this surface $\mu_+ < 0$ and, thus, no Alfvén wave generated in this region can escape from it. Similarly, any Alfvén wave generated in the exterior of the outer critical surface is bound to remain there.

Koide (2003) claimed that in the force-free limit the inner Alfvén surface coincides with the event horizon. This is obviously incorrect due to the property (v) of Appendix A1.

APPENDIX B: BOYER-LINDQUIST AND KERR-SCHILD COORDINATES

In the Boyer-Lindquist coordinates $\{t, \phi, r, \theta\}$ the Kerr metric is

$$ds^2 = g_{tt}dt^2 + 2g_{t\phi}dtd\phi + g_{\phi\phi}d\phi^2 + g_{rr}dr^2 + g_{\theta\theta}d\theta^2, \tag{B1}$$

where

$$g_{tt} = z - 1, \quad g_{t\phi} = -za\sin^2\theta, \quad g_{\phi\phi} = \Sigma\sin^2\theta/\rho^2,$$

$$g_{rr} = \rho^2/\Delta, \quad g_{\theta\theta} = \rho^2,$$

and

$$\begin{aligned} \rho^2 &= r^2 + a^2\cos^2\theta, \\ z &= 2r/\rho^2, \\ \Sigma &= (r^2 + a^2)^2 - a^2\Delta\sin^2\theta, \\ \Delta &= r^2 + a^2 - 2r. \end{aligned}$$

Notice that we use such units where the black hole mass $M = 1$. At the event horizon, where $\Delta = 0$, one has $g_{rr} = \infty$ which is the well know coordinate singularity of the Boyer-Lindquist coordinates. The shift vector is

$$\boldsymbol{\beta} = (g_{t\phi}/g_{\phi\phi}, 0, 0), \tag{B2}$$

so the Boyer Lindquist FIDO is in the state of purely azimuthal motion with constant angular velocity. From (3) one finds that $n_\phi = 0$ and, thus, FIDO is also ZAMO (Zero Angular Momentum Observer, Bardeen at al.,1973.) At the even horizon its world line turns space-like and this is another consequence of the coordinate singularity. This coordinate singularity can be removed via the following integrable coordinate transformation, also singular at the event horizon:

$$\begin{aligned} dt &\rightarrow dt + G(r)dr, \\ d\phi &\rightarrow d\phi + H(r)dr, \end{aligned}$$

where

$$G(r) = -2r/\Delta, \quad H(r) = -a/\Delta.$$

(Since the transformation law for t depends on r this introduces a different foliation of space-time.) The corresponding transformation matrices are

$$\mathcal{A}^{\mu'}_{\mu} = \begin{pmatrix} 1 & 0 & G & 0 \\ 0 & 1 & H & 0 \\ 0 & 0 & 1 & 0 \\ 0 & 0 & 0 & 1 \end{pmatrix}, \tag{B3}$$

$$(\mathcal{A}^{-1})^{\mu}_{\mu'} = \begin{pmatrix} 1 & 0 & -G & 0 \\ 0 & 1 & -H & 0 \\ 0 & 0 & 1 & 0 \\ 0 & 0 & 0 & 1 \end{pmatrix}. \tag{B4}$$

Here we assume that 1) the primed indexes refer to the Boyer-Lindquist coordinates; 2) the upper index indicates the matrix row and the lower index indicates the matrix column. This allows us to apply the Einstein summation rule to the transformation laws, e.g.

$$dx^{\mu'} = \mathcal{A}^{\mu'}_{\mu} dx^{\mu}.$$

In the new coordinates, known as the Kerr-Schild coordinates, the Kerr metric is

$$\begin{aligned} ds^2 = \; & g_{tt}dt^2 + 2g_{t\phi}dtd\phi + 2g_{tr}dtdr + \\ & g_{\phi\phi}d\phi^2 + 2g_{r\phi}d\phi dr + g_{rr}dr^2 + g_{\theta\theta}d\theta^2, \end{aligned} \tag{B5}$$

where

$$g_{tt} = z - 1, \quad g_{t\phi} = -za\sin^2\theta, \quad g_{tr} = z,$$

$$g_{\phi\phi} = \Sigma\sin^2\theta/\rho^2, \quad g_{r\phi} = -a\sin^2\theta(1+z),$$

$$g_{rr} = 1 + z, \quad g_{\theta\theta} = \rho^2.$$

Thus the spatial metric tensor is

$$\gamma_{ij} = \begin{pmatrix} \Sigma\sin^2(\theta)/\rho^2 & -a\sin^2(\theta)(1+z) & 0 \\ -a\sin^2(\theta)(1+z) & 1+z & 0 \\ 0 & 0 & \rho^2 \end{pmatrix}. \tag{B6}$$

As $g_{r\phi} \neq 0$ the spatial coordinates are no longer orthogonal. However, at infinity this tensor has exactly the same form as the metric tensor of Euclidean space in spherical coordinates. This is no surprise as for $r \to \infty$ one has $F(r), H(r) \to 0$ and the Kerr-Schild coordinates become identical to the Boyer-Lindquist coordinates.

The Kerr-Schild lapse function and its shift vector are

$$\alpha = 1/\sqrt{1+z}, \tag{B7}$$

$$\beta^i = (0, \frac{z}{1+z}, 0). \tag{B8}$$

Thus, the Kerr-Schild FIDO is moving radially towards the true singularity at $r = 0$.

It is illuminating to determine the motion of the Kerr-Schild FIDO in the Boyer-Lindquist coordinates. Simple calculations give

$$v^{\phi} = 2ar/\Sigma, \quad v^r = -2r\Delta/\Sigma, \quad v^{\theta} = 0.$$

Thus, the Kerr-Schild FIDO has the same angular velocity as the Boyer-Lindquist FIDO but also moves radially towards the true singularity.

The tensor transformation laws

$$\mathcal{U}_{\mu} = \mathcal{A}^{\mu'}_{\mu}\mathcal{U}_{\mu'}$$

and

$$F_{\mu\nu} = \mathcal{A}^{\mu'}_{\mu}\mathcal{A}^{\nu'}_{\nu}F_{\mu'\nu'}$$

allow us to relate the components of the four-potential and the electromagnetic field tensor in both coordinate systems. It is easy to see that all components of the four potential except $\mathcal{U}_r$ and all components of $F_{\mu\nu}$ with $\mu, \nu \neq r$ are invariant. This immediately shows that the scalar potential $\Phi = -\mathcal{U}_t$, the magnetic flux function $\psi = 2\pi\mathcal{U}_{\phi}$, $H_{\phi} = {}^*F_{t\phi}$ and $E_{\phi} = F_{\phi t}$ are the same in both coordinate systems. Since the angular velocity of magnetic field is given by

$$\Omega = -F_{t\theta}/F_{\phi\theta},$$

it is also invariant.

APPENDIX C: NUMERICAL METHOD

C1 Augmented system of the method of generalized Lagrange multiplier

From eq.(15) one finds

$$\partial_t(\boldsymbol{\nabla}\cdot\boldsymbol{B}) = 0. \tag{C1}$$

This well known result shows that it is sufficient to enforce the divergence free condition (14) only for the initial solution and it will automatically be satisfied at any t. Unfortunately, straightforward applications of many numerical schemes, perfectly suitable for other hyperbolic systems of conservation laws, fail to deliver a good result in the case of electrodynamics and MHD simply because their discrete equations are not consistent with any discrete analogue of (C1). In particular, this applies to the method of Godunov which has many beneficial properties and is currently considered as generally superior to many other numerical schemes for hyperbolic systems. There have been many attempts to find a cure for this "div-B problem", though no perfect solution seems to have been found so far (see the review in Dedner et al.,2002.)

One of the ways to handle this problem involves construction of a somewhat different system of differential equations, the "augmented system", where the divergence free condition (14) is no longer included and $\boldsymbol{\nabla}\cdot\boldsymbol{B}$ may be transported and/or dissipated like other dynamical variables. The idea is not to enforce the divergence free condition exactly but to promote a natural evolution of the system towards a divergence free state. Provided the augmented system is hyperbolic, it can be solved numerically using the Godunov method (Munz et al.2000; Dedner 2002).

Following this idea we propose to modify eq.(8) as follows

$$\nabla_{\beta}\,{}^*F^{\alpha\beta} + \nabla^{\alpha}\Psi + \kappa k^{\alpha}\Psi = 0, \tag{C2}$$

where Ψ is a scalar field which we shell call "the pseudo-potential" and κ =const. As before $k^{\nu} = \partial_t$, where t is the global time coordinate of space-time. From equation (C2) one immediately obtains the evolution equation for Ψ

$$\Box\Psi + \kappa\nabla_t\Psi = 0, \tag{C3}$$

where $\Box = \nabla_{\nu}\nabla^{\nu}$ is the d'Alembert operator. This is the well known "telegraph equation" and it prescribes both propagation and dissipation of Ψ. In fact, $\boldsymbol{\nabla}\cdot\boldsymbol{B}$ is governed by a similar equation. Indeed, from the time component of eq.(C2) one obtains

$$\nabla^t\Psi + \kappa\Psi = \frac{1}{\alpha}\boldsymbol{\nabla}\cdot\boldsymbol{B},$$

whereas from the spatial part one has

$$\nabla_t\left(\frac{\boldsymbol{\nabla}\cdot\boldsymbol{B}}{\alpha}\right) = -\nabla_i\nabla^i\Psi.$$

Combining, these two equations one finds first

$$\nabla^t\nabla_t\left(\frac{\boldsymbol{\nabla}\cdot\boldsymbol{B}}{\alpha}\right) + \kappa\nabla_t\left(\frac{\boldsymbol{\nabla}\cdot\boldsymbol{B}}{\alpha}\right) + \nabla_i\nabla^i(\nabla^t\Psi + \kappa\Psi) = 0$$

and, finally,

$$\Box\left(\frac{\boldsymbol{\nabla}\cdot\boldsymbol{B}}{\alpha}\right) + \kappa\nabla_t\left(\frac{\boldsymbol{\nabla}\cdot\boldsymbol{B}}{\alpha}\right) = 0, \tag{C4}$$

Direct 3+1 splitting of eq.(C2) gives us two conservation laws:

$$\partial_t\left(\sqrt{\gamma}\tfrac{\Psi}{\alpha}\right)+\partial_j\left(\sqrt{\gamma}(B^j-\tfrac{\Psi}{\alpha}\beta^j)\right)=\Psi\left(\kappa\alpha\sqrt{\gamma}-\partial_j(\sqrt{\gamma}\tfrac{\beta^j}{\alpha})\right) \tag{C5}$$

and

$$\partial_t\left(\sqrt{\gamma}(B^i+\tfrac{\Psi}{\alpha}\beta^i)\right)+\partial_j\left(\sqrt{\gamma}(e^{ijk}E_k+\alpha\Psi g^{ij})\right)=\Psi\partial_j(\alpha\sqrt{\gamma}g^{ij}). \tag{C6}$$

Summarizing, we have constructed a system of two vector conservation laws, equations (57,C6), and one scalar conservation law, equation (C5).

C2 Numerical scheme

All 7 evolution equations of the augmented system, as well as the equations of the general relativistic electrodynamics itself, are conservation laws. We can write them as a single abstract vector equation of the form

$$\partial_t(\sqrt{\gamma}\mathcal{Q}^K)+\partial_j(\sqrt{\gamma}\mathcal{F}^{Kj})=\sqrt{\gamma}(\mathcal{S}^K_{(g)}+\mathcal{S}^K_{(d)}), \tag{C7}$$

where

$$\mathcal{Q}^K=\left(\frac{\Psi}{\alpha},B^i+\frac{\Psi}{\alpha}\beta^i,D^i\right) \tag{C8}$$

are the conserved variables, where i is the index of spatial coordinates,

$$\mathcal{F}^{Kj}=\left(B^j-\frac{\Psi}{\alpha}\beta^j,e^{ijk}E_k+\alpha\Psi g^{ij},-e^{ijk}H_k\right) \tag{C9}$$

are the corresponding hyperbolic fluxes,

$$\mathcal{S}^K_{(g)}=\left(-\frac{\Psi}{\sqrt{\gamma}}\partial_k(\sqrt{\gamma}\frac{\beta^k}{\alpha}),\frac{\Psi}{\sqrt{\gamma}}\partial_k(\sqrt{\gamma}\alpha g^{ik}),\rho(-\alpha v^i_d+\beta^i)\right) \tag{C10}$$

are the geometrical source terms, and

$$\mathcal{S}^K_{(d)}=\left(\alpha\kappa\Psi,0^i,-\alpha(\sigma_\parallel D^i_\parallel+\sigma_\perp D^i_\perp)\right) \tag{C11}$$

are the potentially stiff dissipative source terms.

To handle stiff source terms we use the time-step splitting technique (LeVeque 1997). Namely, each time-step we first integrate the truncated system

$$\partial_t(\sqrt{\gamma}\mathcal{Q}^K)+\partial_j(\sqrt{\gamma}\mathcal{F}^{Kj})=\sqrt{\gamma}\mathcal{S}^K_{(g)}, \tag{C12}$$

The result is then considered as the initial solution for another truncated system

$$\partial_t\mathcal{Q}^K=\mathcal{S}^K_{(d)}, \tag{C13}$$

which is integrated over the same time step.

In order to integrate (C12) we apply the Godunov method, slightly modified to accommodate for the spacetime curvature (Pons et al.1998). Integrating (C12) over a spacetime cell ($\Delta t\times\Delta x^1\times\Delta x^2\times\Delta x^3$) one obtains

$$\mathcal{Q}^K(t+\Delta t)=\mathcal{Q}^K(t)-\frac{\Delta t}{\Delta V}\sum_j\mathcal{F}^{Kj}\Delta S_j+\mathcal{S}^K_{(g)}\Delta t, \tag{C14}$$

where the summation is taken over all spatial faces of the cell. In this equation $\mathcal{Q}$ is the vector of conserved variables averaged over the cell volume, $\mathcal{S}_{(g)}$ is the vector of source terms averaged over the cell volume and the time interval, and $\mathcal{F}^{Kj}$ are averaged over the corresponding j-face of the cell and the time interval. If the computational cells are created by coordinate surfaces, as it is in our case, then $\Delta V=\sqrt{\gamma}\Delta x^1\Delta x^2\Delta x^3$ and $\Delta S_i=\pm\sqrt{\gamma}\Delta x^j\Delta x^k$, where $i\neq j\neq k$.

Equation (C14) allows us to advance the numerical solution in time provided $\mathcal{F}^{Kj}$ and $\mathcal{S}_{(g)}$ are known. In the Godunov method, the fluxes $\mathcal{F}^{Kj}$ are found via solving the corresponding Riemann problem at the cell interfaces (LeVeque 1997). Following Pons et al.(1998) we setup such problems utilizing the "primitive" solution vector, $\boldsymbol{P}$, which includes the components $\check{E}^{\hat{i}}=D^{\hat{i}}$ and $B^{\hat{i}}$ of electric and magnetic field as measured in the orthonormal basis of local FIDO, $\boldsymbol{P}^K=(\Psi,B^{\hat{i}},D^{\hat{i}})^t$. This allows us to consider the Riemann problem as observed in the locally inertial frame of the FIDO initially placed at the cell interface and use a special relativistic Riemann solver to find its solution in this frame. At this stage, it is important to take into account the finite speed of the interface relative to FIDO , $\beta^{\hat{i}}$ (Pons et al.1998).

In the locally inertial frame with the Riemann discontinuity normal to the x-axis the relevant system of 1D equations is linear

$$\partial_t\boldsymbol{P}^K+\mathcal{A}^K_L\partial_x\boldsymbol{P}^L=0 \tag{C15}$$

with the Jacobean matrix

$$\mathcal{A}=\begin{bmatrix}0&1&0&0&0&0&0\\1&0&0&0&0&0&0\\0&0&0&0&0&0&-1\\0&0&0&0&0&1&0\\0&0&0&0&0&0&0\\0&0&0&1&0&0&0\\0&0&-1&0&0&0&0\end{bmatrix}.$$

The eigenvalues of this matrix

$$\mu_{(1)}=\mu_{(2)}=\mu_{(3)}=1;$$

$$\mu_{(4)}=0;$$

$$\mu_{(5)}=\mu_{(6)}=\mu_{(7)}=-1$$

provide the wavespeeds of the hyperbolic waves. Other properties of these waves are given by the eigenvectors of $\mathcal{A}$. The right eigenvectors are

$$\begin{aligned}\boldsymbol{r}_{(1)}&=(1,1,0,0,0,0,0)\\\boldsymbol{r}_{(2)}&=(0,0,-1,0,0,0,1)\\\boldsymbol{r}_{(3)}&=(0,0,0,1,0,1,0)\\\boldsymbol{r}_{(4)}&=(0,0,0,0,1,0,0)\\\boldsymbol{r}_{(5)}&=(-1,1,0,0,0,0,0)\\\boldsymbol{r}_{(6)}&=(0,0,1,0,0,0,1)\\\boldsymbol{r}_{(7)}&=(0,0,0,-1,0,1,0)\end{aligned} \tag{C16}$$

Since $\mathcal{A}$ is symmetric, its left eigenvectors, $l^K_{(i)}$, coincide with the corresponding right eigenvectors:

$$l^K_{(i)}=r^K_{(i)}, \tag{C17}$$

It is easy to see that the solutions 2,3,6, and 7 describe the usual electromagnetic waves. The solution 4 simply reflects the fact that all waves of vacuum electrodynamics are transverse and any discontinuity in the normal component of electric field is due to a surface electric charge distribution. the solutions 1 and 5 describe new waves which do not exist in electrodynamics; they transport Ψ and $\boldsymbol{\nabla}\cdot\boldsymbol{B}$ with the speed of light.

The solution to the Riemann problem with the left and the right states, $\boldsymbol{P}_{(l)}$ and $\boldsymbol{P}_{(r)}$, and the interface speed β^x is

$$\boldsymbol{P} = \left\{ \begin{array}{ccc} \boldsymbol{P}_{(l)} & \text{if} & \beta^x < -1; \\ \boldsymbol{P}_{(r)} & \text{if} & \beta^x > +1; \\ \boldsymbol{P}_{(l)} + \sum\limits_{i=1,3} \kappa_{(i)} \boldsymbol{r}_{(i)} & \text{if} & -1 < \beta^x < +1, \end{array} \right. \tag{C18}$$

where

$$\kappa_{(i)} = \frac{(\boldsymbol{P}_{(r)} - \boldsymbol{P}_{(l)}) \cdot \boldsymbol{r}_{(i)}}{\boldsymbol{r}_{(i)} \cdot \boldsymbol{r}_{(i)}}.$$

Notice, that the 4th wave is ignored and the x-component of $\boldsymbol{D}$ is set to be the mean value of the left and the right states

$$D^{\hat{x}} = 0.5(D^{\hat{x}}_{(l)} + D^{\hat{x}}_{(r)}). \tag{C19}$$

In order to make the scheme second order in space and time we introduce slope-limited linear distribution of primitive variables within each cell and use the half-time-step solution following the description in (Falle 1991; Komissarov 1999).

C3 Test simulations

To test the code we carried out a number of test simulations. Here we describe only two of them. In both cases the space-time metric is Minkowskian, so $\boldsymbol{E} = \boldsymbol{D}$ and $\boldsymbol{H} = \boldsymbol{B}$.

The dissipative time scales of our resistivity model is tied to the computational time-step, Δt. Namely, we set

$$\sigma_{\parallel} = d/\Delta t, \tag{C20}$$

and, following the analysis of Sec.2.3, we make the cross field resistivity strongly dependent on $B^2 - D^2$:

$$\sigma_{\perp} = \sigma_{\parallel} \left\{ \begin{array}{ccc} 0 & \text{if} & B^2 \geq D^2 \\ b(D_{\perp} - D^*_{\perp})/D^*_{\perp} & \text{if} & B^2 < D^2 \end{array} \right. , \tag{C21}$$

where $(D^*_{\perp})^2 = B^2 - D^2_{\parallel}$. This model provides continuous $\sigma_{\perp}$ at $D^2 = B^2$ which is preferable for numerical reasons. The corresponding solutions to equations (C13) are

$$D_{\parallel}(t) = D_{\parallel}(0) e^{-\sigma_{\parallel} t}, \tag{C22}$$

and

$$D_{\perp}(t) = D^*_{\perp} + \frac{D^*_{\perp}(D_{\perp}(0) - D^*_{\perp}) e^{-b\sigma_{\parallel} t}}{D_{\perp}(0) + (D^*_{\perp} - D_{\perp}(0)) e^{-b\sigma_{\parallel} t}}. \tag{C23}$$

In fact, each time-step we first evolve $D_{\parallel}$ as in eq.(C22) and then $D_{\perp}$ according to eq.(C23). In most of the problems we use $d \leq 1$ and $b = 0.1$. In addition, we assume that the drift current is described by eq.(100). Although this model resistivity is too high compared to the physical one, any much lower model resistivity would not allow to resolve current sheets (and would become lower that the numerical resistivity.)

C3.1 Alfvén wave

The system of force-free electrodynamics allows two types of hyperbolic waves: 1) the fast waves, which have the same properties as linearly polarized waves of vacuum electrodynamics, and 2) the Alfvén waves, which are similar to the Alfvén waves of relativistic MHD (Komissarov 2002a). The analytical solution for the Alfvén wave used in this test describes a stationary wave with $B_x = B_y = D_z = 1$, $D_y = 0$,

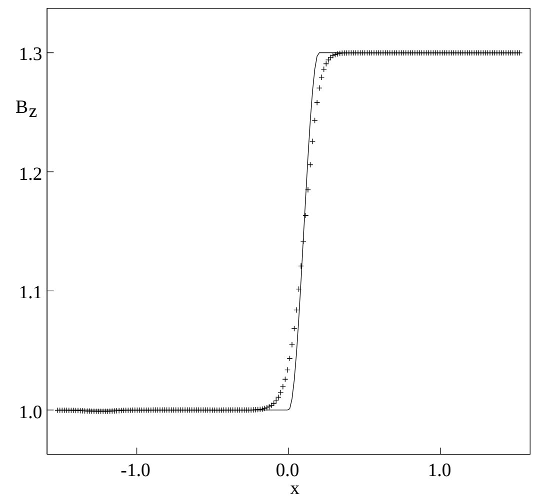

Figure C1. Stationary Alfvén wave. The exact solution and the initial numerical solution are shown by the continuous line. The crosses show the numerical solution at $t = 2$

$$B_z(x) = \left\{ \begin{array}{ccc} 1 & \text{for} & x < 0; \\ 1 + 0.15(1 + \sin 5\pi(x - 0.1)) & \text{for} & 0 < x < 0.2; \\ 1.3 & \text{for} & x > 0.2; \end{array} \right.$$

and

$$D_x = -B_z.$$

The computational grid included 200 identical cells equally spaced between $x = -1.5$ and $x = 1.5$.

Figure C1 shows the solution at $t = 1$. While an electromagnetic wave would cover a distance $\Delta x = 1$ during this time, the Alfvén wave remains stationary and only spreads due to finite resistivity.

C3.2 Current sheet

Here we consider the following Riemann problem:

$$\boldsymbol{D} = 0, \qquad B_z = 0, \qquad B_x = 1$$

$$B_y = \left\{ \begin{array}{ccc} B_0 & \text{for} & x < 0; \\ -B_0 & \text{for} & x > 0; \end{array} \right.$$

The symmetry of this problem implies $B_y = 0$ at the interface at time $t > 0$. If $B_0 < 1$ then this problem has a force-free solution describing two fast waves, switching-off the tangential component of magnetic field and switching-on the z-component of electric field (up to the value of $-B_0$.) In fact, the vacuum electrodynamics has exactly the same solution to this problem. The numerical solution at $t = 1$ for $B_0 = 0.5$ is shown in the panel a) of figure C2. The computational grid is uniform with 200 cells.

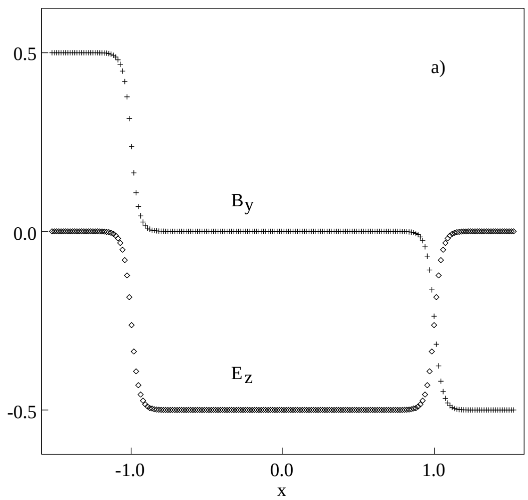

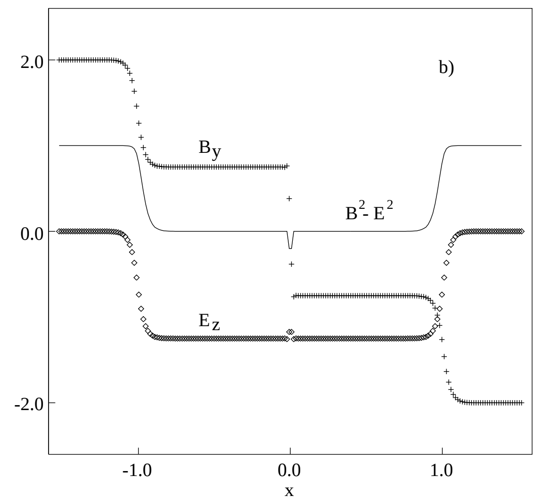

Figure C2. Riemann problem described in Section C3.2. *Left panel:* Numerical solution at $t = 1$ for $B_0 = 0.5$. *Right panel:* Numerical solution at $t = 1$ for $B_0 = 2.0$. The current sheet is located at $x = 0$.

If $B_0 > 1$ then the vacuum electrodynamics still allows solutions of this kind. However, the force-free electrodynamics has no solution in this case because $B^2 - D^2$ vanishes when $|B_y|$ drops down to the value of $(B_0^2+1)/2B_0$. At this point the fast wave is terminated by increased cross-field conductivity that locks $B^2 - D^2$ to 0. Downstream of these waves, the Poynting flux is directed towards the interface located at $x = 0$ where the electromagnetic energy dissipates in a current sheet. The panel b) of figure C2 shows the numerical solution for $B_0 = 2$ at time $t = 1$ on a uniform grid with 200 cells. As expected, the global solution is not sensitive to the exact value of the cross field conductivity which only effect the structure of the current sheet, the higher $\tau_\perp$ leading to the wider current sheet.

REFERENCES

Bardeen J.M., Press W.H., Teukolsky S.A., 1973, ApJ, **178**, 347.

Beskin V.S., Istomin Y.N., Pariev V.I., 1991, Sov.Astron., **36(6)**, 642.

Beskin V.S. and Kusnetsova I.V., 2000, Nuovo Cimento B, **115**, 795.

Bisnovatyi-Kogan G.S., Ruzmaikin A.A., 1976, Astrophys.Sp.Sci., **42**, 401.

Blandford R.D., 1991, in *Physics of Active Galactic Nuclei*, eds. W.J.Duschl and S.J.Wagner, Springer-Verlag, Berlin.

Blandford R.D., 2002, in eds. M.Gilfanov, R.Sunyaev, E.Churazov, *Lighthouses of the Universe: The Most Luminous Celestial Objects and Their Use for Cosmology.* Proc. MPA/ESO, p. 381. (astro-ph/0202265).

Blandford R.D. and Znajek R.L., 1977, MNRAS, **179**, 433.

Boyer R.H., Lindquist R.W., 1967, J.Math.Phys., **8**, 265.

Camenzind M., 1986, A&A, **156**, 137.

Cowling T.G., 1976, "Magnetohydrodynamics", Adam Hilger, London.

Cristodolou D., 1970, Phys.Rev.Lett., **25**, 1596.

Damour T., 1978, Phys.Rev.D, **18**, 3598.

Dedner A., Kemm F., Kröner D., Munz C.-D., Schnitzer T., Wesenberg M., 2002, J.Comp.Phys, **175**, 645.

Ellis G.F.R., 1973, in *Cargése Lectures in Physics*, ed. Schatzman E., Gordon & Breach, New-York, Vol.6, p.1.

Falle S.A.E.G., 1991, MNRAS, **250**, 581.

Goldreich P. and Julian W.H., 1969, Astropys.J., **157**, 869.

Gammie, C.F., McKinney J.C., Tóth G., 2003, ApJ,**589**,444.

Jackson, J.D., 1979, "Classical Electrodynamics", John Wiley & Sons, New York.

Hanni R.S., Ruffini R., 1973, Phys.Rev.D, **8**, 3259.

Hajicek P., 1974, Commune.Math.Phys., **36**, 305

Hirotani K., Okamoto I., 1998, ApJ, **497**, 563.

Jackson, J.D., 1979, "Classical Electrodynamics", John Wiley & Sons, New York.

Kennel C.F., Coroniti F.V., 1984, ApJ, 283, 694

Koide S., 2003, Phys.Rev.D, **67**, 104010.

Komissarov S.S., 1997, Phys.Letters A, **232**, 435.

Komissarov S.S., 1999, MNRAS, **303**, 343.

Komissarov S.S., 2001a, in "Godunov Methods: Theory and Applications", ed. E.F.Toro, Kluwer, New York, p.519.

Komissarov S.S., 2001b, MNRAS, **326**, L41.

Komissarov S.S., 2002a, MNRAS, **336**, 759.

Komissarov S.S., 2002b, in the proceedings of "The 3rd International Sakharov Conference on Physics" held in Moscow, Russia, June 24-29, 2002, eds A.Semikhatov, M.Vasiliev, V.Zaikin, Scientific World Publishing Co., p.392-400; (astro-ph/021114).

Landau L.D., Lifshitz E.M., 1951, *The classical theory of fields*, Addison-Wesley Press, Cambridge, Mass.

Landau L.D., Lifshitz E.M., 1971, *The classical theory of fields*, Addison-Wesley Press, Cambridge, Mass.

LeVeque R.J., 1997, in O.Steiner and A.Gautschy eds., *Computational methods for astrophysical fluid flows*, Springer-Verlag, Berlin.

Macdonald D.A., 1984, MNRAS, **211**, 313.

Macdonald D.A. and Thorne K.S., 1982, MNRAS, **198**, 345.

Mestel L., 1999, "Stellar Magnetism", Clarendon Press, Oxford, p.532.

Michel F.C., 1973, Ap.J.Lett., **180**, L133.

Munz C.-D., Omnes P., Schneider R., Sonnerdrücker, E., Voβ U., 2000, J.Comp.Phys, **161**, 484.

Papadopoulos P., Font J.A., 1998, Phys.Rev.D, **58**, 024005.

Penrose R., 1969, Rev.Nuovo Cim., **1**, 252.

Phinney E.S., 1982, in Ferrari A. and Pacholczyk A.G. eds, *Astrophysical Jets*, Reidel, Dordrecht.

Pons J.A., Font J.A., Ibanez J.M., Martií J.M., Miralles J.A., 1998, A & A, **339**, 638

Punsly B., 1996, ApJ., **467**, 105.

Punsly B., 2001, "Black Hole Gravitohydromagnetics", Springer-Verlag, Berlin.

Punsly B., Coroniti F.V., 1990a, ApJ., **350**, 518.

Punsly B., Coroniti F.V., ApJ., 1990b, **354**, 583.

Takahashi M., Niita S., Tatematsu Y., Tomimatsu A., 1990, ApJ., **363**, 206

Thorne K.S., Price R.H., and Macdonald D.A., 1986, "The Membrane Paradigm", Yale Univ.Press, New Haven.

Thorne K.S., Macdonald D.A., 1982, MNRAS, **198**, 339.

Uchida T., 1997, Phys.Rev.E, **56(2)**, 2181.

Wald R.M., 1974, Phys.Rev D, **10(6)**, 1680.

Weber E.J., Davis L.J., 1967, ApJ, **148**, 217.

Znajek B.L., 1977, MNRAS, **179**, 457.

Znajek B.L., 1978, MNRAS, **185**, 833.